



Title	STUDY OF THE HYDROGENATION AND DOUBLE BOND MIGRATION OF 1-BUTENE ON NICKEL CATALYST
Author(s)	AMENOMIYA, Yoshimitsu
Citation	JOURNAL OF THE RESEARCH INSTITUTE FOR CATALYSIS HOKKAIDO UNIVERSITY, 9(1), 1-41
Issue Date	1961-06
Doc URL	<a href="http://hdl.handle.net/2115/24734">http://hdl.handle.net/2115/24734</a>
Type	bulletin (article)
File Information	9(1)_P1-41.pdf



[Instructions for use](#)

# STUDY OF THE HYDROGENATION AND DOUBLE BOND MIGRATION OF 1-BUTENE ON NICKEL CATALYST<sup>\*)</sup>

By

Yoshimitsu AMENOMIYA<sup>\*\*)</sup>

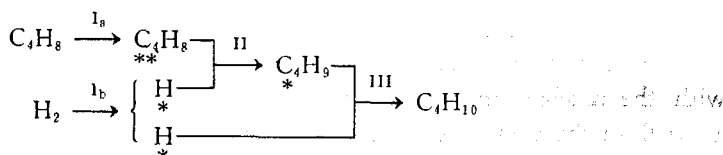
(Received November 10, 1960)

## Abstract

1. The hydrogenation and double bond migration of 1-butene on reduced nickel catalyst were followed by means of gas chromatography over the ranges respectively of the partial pressure of hydrogen from 8 to 50 mmHg and of that of butene from 40 to 180 mmHg mainly at 0°C, and at -30°C, -20°C, 100°C and at 198°C as well. The rate of hydrogenation was thus found to be of the first order in hydrogen and zeroth order in butene at 0°C. The rate of double bond migration was the order of 0.5 and 0.6 with respect to hydrogen and 1-butene respectively at 0°C. The order of reaction of hydrogenation was found unity both for hydrogen and butene at 198°C.

The activation energies of hydrogenation and double bond migration were found to be 11.8 and 7.2 Kcal respectively between -30° and 0°C at *ca.* 40 mmHg hydrogen partial pressure and *ca.* 35 mmHg butene partial pressure. That of hydrogenation was reduced however to -5.6 Kcal at temperatures above 100°C at the same partial pressures of reactants; the appropriate optimum temperature of hydrogenation was estimated at 31°C.

2. The mechanism proposed by HORIUTI and POLANYI (Trans. Faraday Soc., **30**, 663, 1164 (1934)) and developed by HORIUTI (This Journal **6**, 250 (1958) for ethene was extended to butene as :



The structure of the above scheme was constructed according to HORIUTI's method by which the above experimental results were explained semi-quantitatively.

3. The difference of the experimental results of TWIGG (Proc. Roy. Soc., **A 178**, 106 (1941), Disc. Faraday Soc. No. 8, 152 (1950)) and DIBELER and TAYLOR (J. Phys. Chem., **55**, 1036 (1951)) from those of the present author in the order of reaction and activation energies was accounted for with reference to the location of temperature range of measurement relative to

<sup>\*)</sup> This work was reported in *Shokubai (Catalysis)*, Vol. 2, No. 1 P. 1 (1960) in Japanese.

<sup>\*\*)</sup> Tokyo Institute of Technology, Meguroku, Tokyo, Japan, present address: National Research Council, Ottawa, Canada.

the optimum temperature mentioned in 1. in the light of the above structure.

It was further predicted that at sufficiently low temperature the activation energy should be the same for hydrogenation of every olefin on the nickel catalyst.

## Introduction

The hydrogenation of olefins over reduced metal catalysts have been studied by many investigators and various mechanisms for this catalytic reaction have been proposed by them. Exchange reaction with deuterium and isomerization of higher olefins which take place simultaneously with hydrogenation have been increasingly studied along with the recent development of analytical methods.

The isomerization associated with the catalyzed hydrogenation in the presence of nickel catalyst was first reported by TWIGG<sup>1)</sup> in 1941. Since then, the isomerization of butene was investigated by TWIGG<sup>2)3)</sup> himself and DIBELER and TAYLOR<sup>4)</sup> together with exchange reaction using a nickel filament as catalyst, and they found the same order of reaction for hydrogenation and double bond migration (abbreviated to DBM in what follows), that is, the order of reaction of 1/2 with respect both to hydrogen and 1-butene partial pressures in either case. The activation energies of the exchange, hydrogenation and DBM were determined respectively as 9.0, 2.5 and 5.9 Kcal by TWIGG<sup>2)</sup> over the temperature range between 76 and 126°C, and as 7.1, 2.0 and 5.0 Kcal by DIBELER and TAYLOR<sup>4)</sup> over the temperature range between 60 and 135°C.

The isomerization as well as the exchange is expected of course to provide important informations for elucidating the mechanism of the hydrogenation of olefin. However, the order of reaction observed by TWIGG<sup>2)</sup> and DIBELER and TAYLOR<sup>4)</sup> were not accounted for by the mechanisms so far proposed inclusive of that advanced by TWIGG<sup>3)</sup> himself.

HORIUTI and POLANYI<sup>5)6)</sup> concluded the mechanism of catalyzed hydrogenation of olefins in the presence of metallic catalysts and suggested in accordance with the mechanism that the hydrogenation should be accompanied by DBM as well as the exchange reaction as verified later by TWIGG *et al.* HORIUTI<sup>7)8)</sup> formulated the mechanism statistical mechanically and accounted for the experimental results of ZUR STRASSEN<sup>9)</sup>, concluding that the rate-determining step of hydrogenation was the adsorption of hydrogen on the surface at lower temperature but the combination of adsorbed ethyl radical with adsorbed hydrogen atom at higher temperature; the optimum temperature of hydrogenation was thus accounted for as the temperature, where the rate-determining step switched over from one to the other. Analogical extension of the mechanism to higher olefins predicts that the optimum temperature decreases with increase of molecular weight of olefins as shown in §18. Hence it is possible that TWIGG and

DIBELER and TAYLOR have determined the activation energy over a temperature range around the optimum temperature, where very small or even negative activation energy and a fractional order of reaction are expected as deduced in § 18.

The analogical extension of the mechanism leads to the conclusion, on the other hand, that the activation energy of hydrogenation on nickel catalyst must be common to olefins at sufficiently low temperature, where the adsorption of hydrogen determines rate. However, TWIGG obtained 8.2, 6.0, 3.3 and 3.3 kcal as the activation energies of the catalyzed deuteration of ethene, propene, 2-butenes and *iso*-butene respectively over the temperature range from 55 to 120°C in the presence of nickel filament. This indicates again that the temperature range of the observation was around the optimum temperature, since then the observed activation energy should decrease as the optimum temperature shifts from higher to lower temperature with increase of the molecular weight of olefin.

The present work has been devoted to the experimental investigation of the hydrogenation and DBM of 1-butene in the presence of nickel catalyst with particular stress on that at low temperature with the purpose of elucidating the above subject in question. Isomers of butene were analyzed by means of gas chromatography. The experimental results were analyzed for the rate of DBM by a different method from that of TWIGG *et al*<sup>(4)</sup>, which did not require 100% of 1-butene as material.

## Chapter I. Experimental

### § 1. Catalyst

The catalyst was about 5% nickel by weight supported on  $\alpha$ -alumina. The  $\alpha$ -alumina was prepared by heating activated alumina (200 mesh) of WAKO Pure Chemicals Ltd., Tokyo, for 2 hrs at 1300°C, and checked by X-ray diffraction for the absence of  $\gamma$ -alumina. Nickel was precipitated by ammonium carbonate from nickel nitrate solution in which  $\alpha$ -alumina was suspended. The above nickel solution was prepared by dissolving metallic nickel of International Nickel Corp. in pure nitric acid. The precipitate was heated on a water bath for 30 min, filtered, washed, pelleted and dried at 110°C. The pellet of catalyst was broken to small pieces for use.

### § 2. Reactants

Cylinder hydrogen was purified by passing it through calcium chloride, palladium asbestos at 350°C, sodium hydroxide, and liquid nitrogen trap to

remove a trace of water.

Butenes were prepared by dehydration of *n*-butyl alcohol over plain alumina or alkali added alumina. Butene mixture which contained 30-50% 2-butenes was prepared with plain alumina kept at 350°C at LHSV (liquid hourly space velocity) below 0.6. Another mixture which contained more than 90% 1-butene was obtained with alkali added alumina (3% alkali) kept at 350°C at *ca.* 1.0 LHSV<sup>10</sup>.

Butene mixtures prepared as above were dried over sodium hydroxide, twice distilled into dry ice-alcohol trap and evacuated, and finally condensed in liquid nitrogen trap and evacuated. These mixtures contained less than 1% of impurities consisting of C<sub>2</sub> and C<sub>3</sub> hydrocarbons and butane, which were neglected in calculating the compositions of butene mixtures.

### § 3. Apparatus and Experimental Method

The apparatus was made of hard glass as illustrated in Fig. 1. The reaction system incorporated an U-shaped reactor and a circulating pump of centrifugal type which was operated by an outside magnet. The gas was circulated rapidly in the reaction system through C, W, T<sub>1</sub> and R to prevent the reaction from being controlled by diffusion. The inlet side of the reactor was given of zigzag shape as shown in Fig. 2, lest the catalyst should be cooled by the rapid flow of gas.

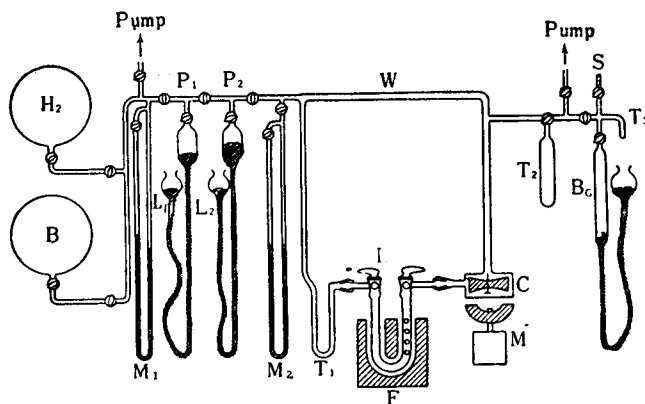


Fig. 1. Apparatus.

H <sub>2</sub> : Reservoir of hydrogen	C: Circulation pump
B: Reservoir of butene	M: Motor
M <sub>1</sub> , M <sub>2</sub> : Manometer	B <sub>c</sub> : Gas burette
P <sub>1</sub> , P <sub>2</sub> : Gas pipette	S: Serum pipette
R: Reactor	F: Furnace or bath
T <sub>1</sub> , T <sub>2</sub> , T <sub>3</sub> : Liquid nitrogen trap	

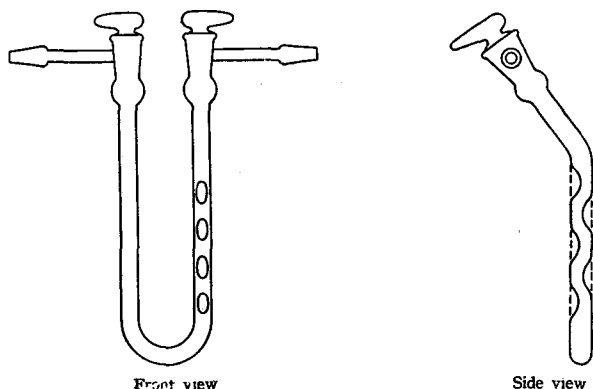


Fig. 2. Reactor.

The catalyst was placed at the bottom of the reactor R, which was heated by an aluminum block furnace or a glycerin bath. The temperature of the furnace or the bath was controlled by an electronic controller and measured by a chromel-alumel thermocouple inserted in the block or the bath. The volume of the reactor was about 30 cc. Two kinds of the reaction system were employed; one of them had the volume of about 220 cc and the other about 360 cc. The latter reaction system was used only for the measurement of activation energies.

Before use the catalyst was heated up to 400°C *in vacuo*, and reduced with 500 mmHg of purified hydrogen circulated over the catalyst for 2 hrs at the same temperature. A trace of water produced by reduction was removed by the liquid nitrogen trap T<sub>1</sub>. The pressure decrease of hydrogen could not be observed practically after the first 30 minutes. The catalyst thus reduced was now evacuated to 10<sup>-2</sup>-10<sup>-3</sup> mmHg for 30 minutes at 400°C, and left to cool to the temperature of a run.

A run was conducted as follows. Hydrogen and butene were measured manometrically in the pipette P<sub>1</sub> and P<sub>2</sub> respectively and mixed. The mixture was introduced into the evacuated reaction system W, T<sub>1</sub> and C in Fig. 1, and the run was started by opening the taps of the evacuated reactor R after the pump was set operating.

The hydrogenation was followed by the total pressure by means of the manometer<sup>\*)</sup> M<sub>2</sub>. The ratio of the total pressure in the system W, C and T<sub>1</sub>

\*) The amount of *n*-butane produced was determined both by the decrease of total pressure and the gas chromatographic analysis. Both the values agreed with each other within experimental error, whereas the former procedure was generally practiced. This evidences on the other hand that no other reaction than hydrogenation and DBM occurred. Further evidence of the latter conclusion is provided by the gas-chromatographic data that no formation of higher or lower hydrocarbon than those of C<sub>4</sub> was detected except at higher temperatures above 120°C.

before communicating R, to that after the communication was preliminarily determined at each reaction temperature using hydrogen. The initial total pressure of the run was calculated by dividing the pressure in W, C and T<sub>1</sub> observed before the communication by the above ratio. After a recorded time the reaction was stopped by closing the taps of R. The resultant gas in W, C and T<sub>1</sub> was led to the liquid nitrogen trap T<sub>2</sub> and uncondensable gas was pumped off. The condensable component was now transferred by distillation into T<sub>3</sub> and then collected in B<sub>G</sub> by evaporation. A portion of the gas in B<sub>G</sub> was taken out through the serum cap S by a small syringe and analyzed by means of gas chromatography.

After the run the catalyst was evacuated for 20 minutes at the reaction temperature and left at room temperature with 300 mmHg of hydrogen. Just before the next run the catalyst was kept at 390°C for 20 minutes in the same hydrogen and then evacuated for 30 minutes at the same temperature.

The efficacy of circulation was checked beforehand as follows. It was observed that the reaction rate increased with pump speed (rpm) below a certain critical value but not beyond it and that the critical value increased with increase of the amount of catalyst. Rates were measured at sufficiently high pump speed above the critical value.

TABLE I. Contents of butenes before and after circulation

No. of Runs	Circulation time (min)	Content of butenes		Difference
		initial (%)	final (%)	
114	6	91.77	91.43	- 0.34
115	7.5	90.30	89.49	- 0.81
116	14.5	90.32	90.05	- 0.27
117	39	86.21	85.37	- 0.84
118	11	78.93	78.58	- 0.35
119	8.3	70.85	70.53	- 0.32
120	13.5	85.58	85.81	+ 0.23
121	29	81.65	81.58	- 0.07
127	9.3	88.81	88.69	- 0.12
158	1	90.60	90.30	- 0.30

Dissolution of butenes into grease was also preliminarily investigated. Table 1 shows the results of an experiment in which a mixture of butenes and hydrogen was circulated in the reaction system for several minutes. The initial or the final content of butenes in the mixture is shown in the third or the fourth

column respectively of the Table. The difference between the initial and final butene content in the mixture was so small that the dissolution of butenes into grease could be neglected.

#### § 4. Analysis

The analysis of reactant and resultant gas was conducted at room temperature by means of a home-made gas chromatographic apparatus of thermal conductivity type with platinum filaments in conductivity cell using columns of dimethyl formamide on alumina (7-9 m) or triisobutylene on celite (5 m) and dioctyl phthalate on celite (3 m) in series. Hydrogen was employed as carrier gas, and the composition of gas was determined directly from the areas of chromatogram without correction. This procedure is justified by the coincidence of the quantity of butane thus determined with that observed by manometer.

### Chapter II. Results

#### § 5. Hydrogenation

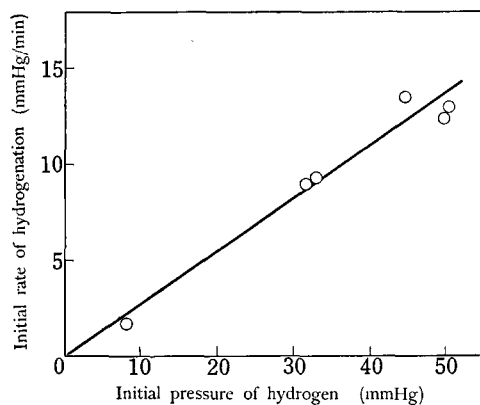
Hydrogenation rate was found to vary so slowly with the lapse of time in each run that its extent in the first minute could be practically taken as the initial rate of hydrogenation.

Table 2 and Fig. 3 show the results obtained by maintaining butene pressure constant (about 94 mmHg) and varying hydrogen pressure from 8 to 50 mmHg at 0°C. The activity of catalyst did not run down in this experiment conducted at comparatively high partial pressure of hydrogen. The initial rate determined as above was plotted against the partial pressure of hydrogen in Fig. 3, which showed that the rate of hydrogenation was proportional to the partial pressure

TABLE 2. Effect of hydrogen pressure on the rate of hydrogenation  
temperature: 0°C, catalyst: 0.042 g.

No. of Runs	Initial hydrogen pressure (mmHg)	Initial butene pressure (mmHg)	Initial rate (mmHg/min)
166	44.5	94.1	13.5
167	8.0	94.5	1.7
169	50.1	93.7	13.1
170	49.7	94.7	12.4
171	32.7	94.2	9.3
172	31.4	93.8	9.0

of hydrogen. The reactant hydrocarbon in the above experiment contained 91.1% of 1-butene, 1.4% of *trans*-2-butene, 3.1% of *cis*-2-butene, and 4.4% of *n*-butane.



**Fig. 3.** Initial rate of hydrogenation~hydrogen pressure.  
catalyst: 0.042 g, temperature: 0°C,  
initial pressure of butene: 93.7~94.7 mmHg

Table 3 and Fig. 4 show the results obtained by maintaining hydrogen partial pressure constant at about 19 mmHg and by varying butene partial pressure from 40 to 180 mmHg at 0°C. Some deactivation of the catalyst was observed in the course of this experiment. The effect of butene partial pressures on the rate of hydrogenation was deduced under the circumstances as follows

**TABLE 3.** Effect of butene pressure on the rate of hydrogenation  
temperature: 0°C, catalyst: 0.071 g

No. of Runs	Initial butene pressure (mmHg)	Initial hydrogen pressure (mmHg)	Initial rate (mmHg/min)	Mean initial rate (mmHg/min)
159	40.4	18.7	10.6	9.1
164	40.6	18.9	7.5	
160	83.3	19.1	11.6	9.3
163	82.0	22.6	7.1	
161	124.5	18.4	8.9	8.5
162	123.4	18.8	8.1	
158	179.7	19.3	8.0	5.9
165	181.8	19.4	3.7	

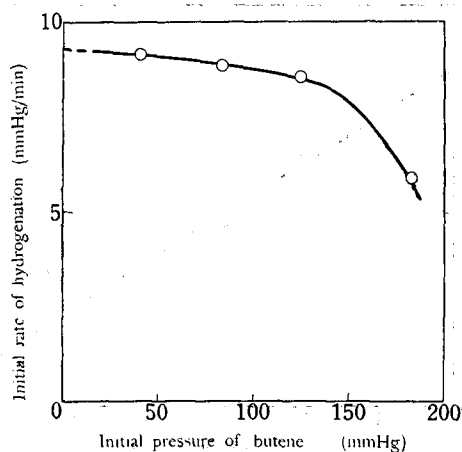


Fig. 4. Initial rate of hydrogenation ~ butene pressure.  
catalyst: 0.071 g, temperature: 0°C,  
initial pressure of hydrogen: 19 mmHg.

from the results of a series of runs conducted at a similar condition except in the partial pressure of butene. Those pairs of runs were picked up from the series, as shown in Table 3, which had equal sum of numbers of the runs in the series and each consisted of runs of approximately equal initial partial pressures respectively of butene and hydrogen (*ca.* 19 mmHg). The mean initial rate of each pair was now taken as appropriate to the respective means of butene partial pressures, free from the effect of the deactivation of catalyst, and plotted against the latter as shown in Fig. 4. The Figure shows that the rate of hydrogenation is approximately independent of the partial pressure of butene below 120 mmHg, but strongly retarded by butene above 120 mmHg. The composition of the reactant hydrocarbon in the above experiment was 67.4% of 1-butene, 18.5% of *trans*-2-butene, and 14.1% of *cis*-2-butene.

It follows that the rate  $r_h$  of hydrogenation is expressed for butene partial pressure below 120 mmHg, as

$$r_h = k_h P^H \quad (P^B < 120 \text{ mmHg}), \quad (5.1)$$

where  $P^H$  and  $P^B$  are the partial pressures of hydrogen and butene respectively and  $k_h$  a constant. This indicates that the surface of the catalyst is practically unoccupied by butene under the pressures below 120 mmHg.

Fig. 5 shows  $\log P^H$  of a single run plotted against time. The excellent linearity obtained is in conformity with (5.1) alternatively induced from the observation of initial rates.

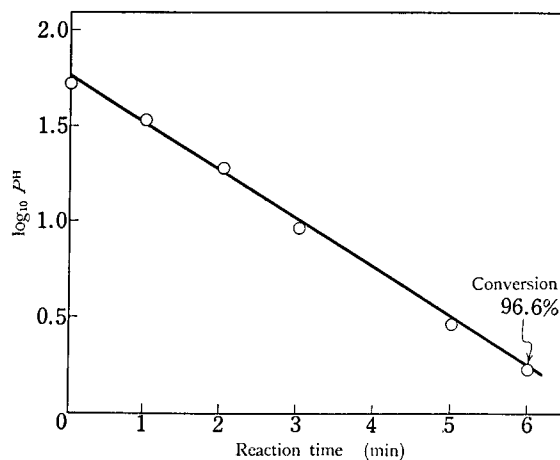


Fig. 5.  $\log P^H \sim t$ .

catalyst: 0.145 g, temperature: 0°C, initial pressure of hydrogen: 51.6 mmHg, initial pressure of butene: 78.0 mmHg, butane produced: 49.9 mmHg (conversion of hydrogen: 96.6%)

### § 6. DBM (Double Bond Migration)

The results of experiments on DBM are shown in Table 4, where the notations are defined as

- $P^H$  : partial pressure of hydrogen
- $P^B$  : partial pressure of total butenes
- $P^{1-B}$  : partial pressure of 1-butene
- $P^{t-B}$  : partial pressure of *trans*-2-butene
- $P^{c-B}$  : partial pressure of *cis*-2-butene
- $P^{n-B}$  : partial pressure of *n*-butane

and their initial values are designated by suffix 0. We have by definition

$$P^B := P^{1-B} + P^{t-B} + P^{c-B}$$

$$P_0^B = P_0^{1-B} + P_0^{t-B} + P_0^{c-B}.$$

Groups I, II *etc.* in Table 4 refer each to a number of runs which were conducted at approximately the same initial partial pressures of hydrogen and butene but for different reaction time. The increase  $\Delta P^{n-B}$  of  $P^{n-B}$  was measured several times during the run by the decrease of total pressure, although the Table shows just  $\Delta P^{n-B}$  at the reaction time *i.e.* at the end of the run; the increase  $\Delta P^{1-B}$ ,  $\Delta P^{t-B}$  and  $\Delta P^{c-B}$  respectively of  $P^{1-B}$ ,  $P^{t-B}$  and  $P^{c-B}$ , shown in the Table are those at the reaction time, too, as determined by gas chromatographic analysis of the resultant gas of the run.

TABLE 4. Double bond migration  
temperature: 0°C, catalyst: 0.030 g

Group	No. of Runs	Initial hydrogen pressure $P_0^H$ (mmHg)	Initial total pressure of butenes $P_0^B$ (mmHg)	Initial 1-butene pressure $P_0^{1-B}$ (mmHg)	reaction time (min)	Increase of component				$-(dP^H/dt)_0$ mmHg/m n)	$-dP^{1-B}/dt)_0$ (mmHg/min)	$\frac{(dP^{1-B}/dt)_0}{(dP^B/dt)_0}$
						$\Delta P^{n-B}$ (mmHg)	$\Delta P^{1-B}$ (mmHg)	$\Delta P^{t-B}$ (mmHg)	$\Delta P^{c-B}$ (mmHg)			
I	204	24.7	25.2	23.3	2	+ 1.8	- 2.0	+ 0.2	- 0.1	4.9	5.4	1.11
	205	24.4	25.5	23.5	3	+ 4.6	- 4.5	0	- 0.1			
II	213	24.6	45.1	41.6	1	+ 2.7	- 3.0	+ 0.2	+ 0.2	12.3	16.4	1.33
	211	25.0	45.4	41.9	0.75	+ 8.9	- 11.3	+ 1.7	+ 0.8			
	208	24.7	45.5	42.0	1	+ 10.6	- 12.9	+ 1.7	+ 0.5			
	200	25.0	45.1	41.6	2	+ 13.2	- 13.6	+ 0.8	- 0.3			
III	212	24.8	69.9	64.5	1	+ 11.7	- 16.7	+ 3.4	+ 1.6	16.0	26.1	1.63
	210	24.6	69.9	64.5	2	+ 18.3	- 27.9	+ 6.5	+ 3.1			
IV	203	25.1	100.1	92.4	1	+ 4.8	- 7.7	+ 1.7	+ 1.1	11.2	20.9	1.87
	202	25.1	100.0	92.3	1.56	+ 12.5	- 18.0	+ 4.0	+ 1.5			
V	218	10.4	99.8	92.1	2	+ 3.0	- 8.7	+ 3.3	+ 2.5	6.0	13.3	2.22
	219	10.4	100.0	92.3	5	+ 5.1	- 14.3	+ 5.3	+ 4.0			
VI	221	37.7	100.4	92.7	1	+ 12.5	- 16.1	+ 2.2	+ 1.5	13.1	19.5	1.49
	220	37.9	99.7	92.0	2	+ 17.8	- 22.2	+ 2.9	+ 1.5			
VII	217	63.0	100.1	92.4	0.75	+ 11.3	- 13.9	+ 1.3	+ 1.3	15.6	22.0	1.41
	222	63.5	101.3	93.5	2	+ 26.3	- 28.6	+ 2.0	+ 0.3			

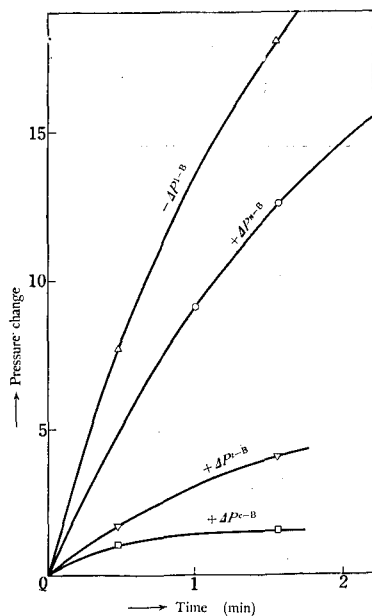


Fig. 6. Pressure change of butane and butenes with time.

catalyst: 0.030 g, temperature: 0°C,  
 $P_0^H = 25.1$  mmHg,  $P_0^B = 100$  mmHg.

It follows that DBM proceeds simultaneously with hydrogenation, from the result shown in Fig. 6 that 2-butenes increase at the initial stage of the reaction in spite of the decrease of the total amount of butenes.

The content of 1-butene in the reactant is however in excess over that in

TABLE 5. Composition of reactant and equilibrium composition\* at 0°C.

	Reactant (%)	Equilibrium (%)
1-butene	92.3	2.0
<i>trans</i> -2-butene	2.1	78.4
<i>cis</i> -2-butene	4.5	19.6
<i>n</i> -butane	1.1	
Total	100.0	100.0

\* Equilibrium composition was calculated from *Selected Values of Physical and Thermodynamic Properties of Hydrocarbons and Related Substances*. Rossini, Carnegie Press, 1953.

Fig. 6 shows  $\Delta P^{n-B}$  etc. increasing with time of group IV in Table 4 as an example. The curve of  $\Delta P^{2-B}$  of run No. 202 was first drawn from data not fully given in Table 4; those of  $\Delta P^{1-B}$ ,  $\Delta P'^{2-B}$  and  $\Delta P^{2-B}$  were now constructed by plotting  $-\Delta P^{1-B}$  etc. of run No. 202 against the reaction time given in Table 4 and those of run No. 203 against the time, which corresponds, in accordance with the curve of  $\Delta P^{n-B}$  drawn as above, to the magnitude of  $\Delta P^{n-B}$  of run No. 203. This procedure is based on the assumption that the ratio of the activity of DBM to that of hydrogenation remains constant, if the activities themselves were varied. The initial rates  $-(dP^H/dt)_0$  and  $-(dP^{1-B}/dt)_0$  of hydrogenation and the decrease of 1-butene are determined, as shown in Table 4, respectively as the initial slopes of  $\Delta P^{n-B}$ - and  $\Delta P^{1-B}$ -curves thus constructed as exemplified with reference to Fig. 6.

TABLE 6. Reaction of 1-butene on reduced nickel in the absence of hydrogen

temperature: 0°C, catalyst: 0.057 g, reaction time: 45 min, no pressure change was observed

	Reactant (mmHg)	Product (mmHg)
1-butene	142.9	143.8
<i>trans</i> -2-butene	54.1	52.7
<i>cis</i> -2-butene	44.7	45.2
<i>n</i> -butane	0	0
Total	241.7	241.7

equilibrium at 0°C as shown in Table 5, which affirms the thermodynamic feasibility of DBM to proceed. Table 6 shows the result of a run in the presence of reduced nickel at 0°C that DBM did not proceed in the absence of hydrogen within the experimental error of gas chromatographic analysis, in conformity with that of TWIGG<sup>2)</sup> or DIBELER and TAYLOR<sup>4)</sup>. Table 7 shows the result of a run of 1-butene and hydrogen in contact with  $\alpha$ -alumina, that neither hydrogenation nor DBM was catalyzed by  $\alpha$ -alumina *i. e.* the supporter of nickel. It is hence concluded from the present experiment, that DBM is catalyzed by nickel in the presence of hydrogen.

TABLE 7. Reaction of the mixture of hydrogen and 1-butene on  $\alpha$ -alumina

temperature: 0°C,  $\alpha$ -alumina: 0.704 g, reaction time: 10 min, partial pressure of hydrogen: 28.8 mmHg, no pressure change was observed.

	Reactant (mmHg)	Product (mmHg)
1-butene	56.3	56.5
<i>trans</i> -2-butene	2.8	2.7
<i>cis</i> -2-butene	3.2	3.2
<i>n</i> -butane	0.6	0.5
Total	62.9	62.9

The order of reaction of DBM with respect to butene was determined from the results at constant hydrogen partial pressure of about 25 mmHg and at different butene partial pressure at 0°C, which were picked up from Table 4 as

shown in Table 8. The consistent value of  $(dP^{1-B}/dt)_0$  unaffected by the change of catalytic activity should be obtained by multiplying  $(dP^{1-B}/dt)_0/(dP^H/dt)_0$ , unaffected as assumed above by similarly unaffected value of  $(dP^H/dt)_0$ .

TABLE 8. Effect of 1-butene pressure on the rate of decrease of 1-butene

temperature: 0°C, catalyst: 0.030 g

No. of Runs	Initial hydrogen pressure $P_0^H$ (mmHg)	Initial 1-butene pressure $P_0^{1-B}$ (mmHg)	$\sqrt{P_0^{1-B}}$ mmHg <sup>1/2</sup>	$\frac{(dP^{1-B}/dt)_0}{(dP^H/dt)_0}$ (a)	Correction factor of activity (b)	$r=(a)\times(b)$
204, 205	24.5	23.4	4.84	1.11	0.989	1.10
200, 208 211, 213	24.8	41.8	6.47	1.33	0.979	1.30
210, 212	24.7	64.5	8.03	1.63	0.968	1.58
202, 203	25.1	92.3	9.61	1.87	0.946	1.77

The value of  $(dP^H/dt)_0$ , from which the effect of change of catalytic activity was eliminated as in § 5, is shown in Table 3 and Fig. 4. The corrected value of  $(dP^H/dt)_0$  decreases slightly with increase of butene partial pressure even below 120 mmHg as seen from Fig. 4. Table 8 shows the ratio (b) of the value of  $(dP^H/dt)_0$  to that at zero butene partial pressure as derived from the result of Fig. 4. The product  $r$  of (b) and (a)  $\equiv (dP^{1-B}/dt)_0/(dP^H/dt)_0$  shown in Table 8 is now the fraction of  $(dP^{1-B}/dt)_0$  over  $(dP^H/dt)_0$  at  $P^B=0$  unaffected by the change of catalytic activity.

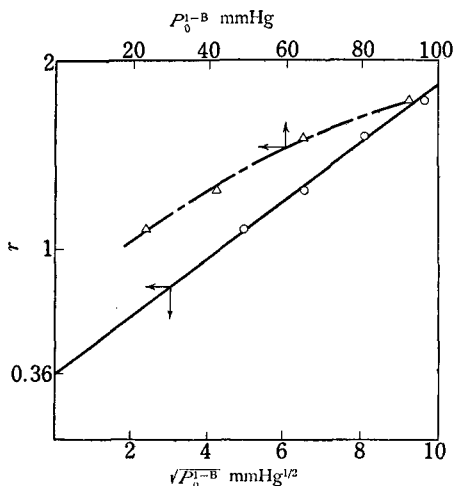


Fig. 7.  $r \sim P_0^{1-B}$  and  $r \sim \sqrt{P_0^{1-B}}$   
temperature: 0°C

The product  $r$  is plotted in Fig. 7 against  $P_0^{1-B}$  as well as its square root, which shows that  $r$  varies linearly with  $\sqrt{P_0^{1-B}}$ . The intercept 0.36 of the straight line of  $r$  vs  $\sqrt{P_0^{1-B}}$  on the ordinate gives now the ratio of the hydrogenation rate of 1-butene to that of total butenes. Admitting that the hydrogenation rate is approximately constant independent of  $P^B$  or  $P^{1-B}$ , the excess  $r_m$  of  $r$  over 0.36 should be the rate of DBM, which is proportional to the square root of 1-butene pressure, *i. e.*

$$r_m \propto (P^{1-B})^{0.5} \quad (6.1)$$

The order of reaction of DBM

TABLE 9. Effect of hydrogen pressure on  $r_m$   
 temperature: 0°C, catalyst: 0.030 g

No. of Runs	$P_0^H$ mmHg	$P_0^B$ mmHg	$r_h$ mmHg/min	$\frac{(dP^{1-B}/dt)_0}{(dP^H/dt)_0}$	$-(dP^{1-B}/dt)_0$ (a) mmHg/min	$r_h \times 0.36$ (b) mmHg/min	$r_m = (a) - (b)$ mmHg/min
218, 219	10.4	99.9	2.56*	2.22	5.68	0.92	4.76
202, 203	25.1	100.0	6.17*	1.87	11.54	2.22	9.32
220, 221	37.8	100.1	9.30*	1.49	13.90	3.34	10.56
217, 222	63.3	100.7	<b>15.60</b>	1.41	22.00	5.61	16.39

\* Calculated from (5-1) and 15.60 mmHg/min at  $p_0^H = 63.3$  mmHg.

with respect to hydrogen partial pressure was now deduced as follows from the results at constant butene partial pressure (about 100 mmHg) and hydrogen partial pressure ranging from 10 to 63 mmHg at 0°C, which were picked up from Table 4 as shown in Table 9. The upper three data in the column of  $r_h$  in Table 9 were calculated on the base of  $k_h$  in (5.1) appropriate to the value of  $r_h$  in the last row. These values of  $r_h$  are multiplied by  $(dP^{1-B}/dt)_0 / (dP^H/dt)_0$  to obtain the rate  $-(dP^{1-B}/dt)_0$  of decrease of 1-butene at the constant catalyst activity as shown in the third last column of the Table. Subtracting from the latter value of the overall rate  $-(dP^{1-B}/dt)_0$  of decrease of 1-butene, the rate 0.36  $r_h$  of its decrease due to hydrogenation, the rate  $r_m$  of DBM is determined as:

$$r_m = \frac{(dP^{1-B}/dt)_0}{(dP^H/dt)_0} r_h - 0.36 r_h \quad (6.2)$$

as shown in the last column of Table 9. The plot of  $\log r_m$  against  $\log P_0^H$  shown in Fig. 8 yields a straight line with the slope of 0.6.

We have thus in conclusion

$$r_m = k_m (P^H)^{0.6} (P^{1-B})^{0.5} \quad (6.3)$$

where  $k_m$  is the appropriate rate constant.

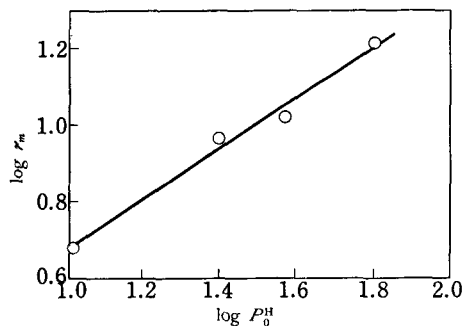


Fig. 8.  $\log r_m \sim \log P_0^H$ .  
 temperature: 0°C

### § 7. Temperature Dependence of Reaction Rate

Table 10 shows the initial rate of hydrogenation observed at different temperatures between -30 and 198°C. The directly observed value of the initial rate given in the third last column of the Table was corrected for the

TABLE 10. Rate of hydrogenation

catalyst: 0.023 g,  $f=1.0759$ .

No. of Runs	Temperature (°C)	$p_0^H$ (mmHg)	$p_0^B$ (mmHg)	Initial rate (mmHg/min)	$f^n$	Corrected initial rate (mmHg/min)
269	0	39.7	34.7	5.9	1.00	(5.9)
271	— 33	39.3	33.6	0.2	1.16	0.23
272	0	39.3	34.4	3.9	1.25	4.9
273	— 33	39.3	34.4	0.2	1.35	0.27
274	— 19.5	39.3	34.5	0.9	1.45	1.3
275	0	39.8	34.8	3.6	1.56	5.6
276	— 19.5	39.6	34.5	0.9	1.68	1.5
277	0	40.0	35.0	2.9	1.81	5.2
278	120	40.5	34.9	4.1	1.95	8.0
279	198	40.6	35.5	1.1	2.10	2.3
280	100	40.6	35.1	4.3	2.26	9.7
281	— 20.7	39.1	34.3	0.5	2.43	1.2

regular deactivation of the catalyst by multiplying by  $f^n$ , where  $n$  was the number of run and  $f$  the factor of deactivation for a run, which was fitted to several measurements of the initial rate at 0°C (Nos. 269, 272, 275 and 277) inserted here and there in the series. of runs. The initial rates thus corrected are shown in the last column of Table 10 and plotted against the reciprocal of absolute temperature in Fig. 9.

Table 11 shows  $(dP^{1-B}/dt)_0$  which was measured simultaneously with  $r_h$  in the runs given in Table 10 at 0 and *ca.*  $-20^\circ\text{C}$ , the appropriate value of  $(dP^{1-B}/dt)_0/(dP^H/dt)_0$  and that of  $r_m$  calculated from them by (6.2). The value of  $r_m$  is plotted in Fig. 9 as shown by a chain line.

TABLE 11. Temperature dependence of  $r_m$

catalyst: 0.023 g

No. of Runs	Temperature (°C)	$\frac{(dP^{1-B}/dt)_0}{(dP^H/dt)_0}$	$r_h$ (mmHg/min)	$r_m$ (mmHg/min)
275	0	1.15	5.6	4.4
277	0	1.15	5.2	4.1
276	— 19.5	1.39	1.5	1.6
281	— 20.7	1.42	1.2	1.3

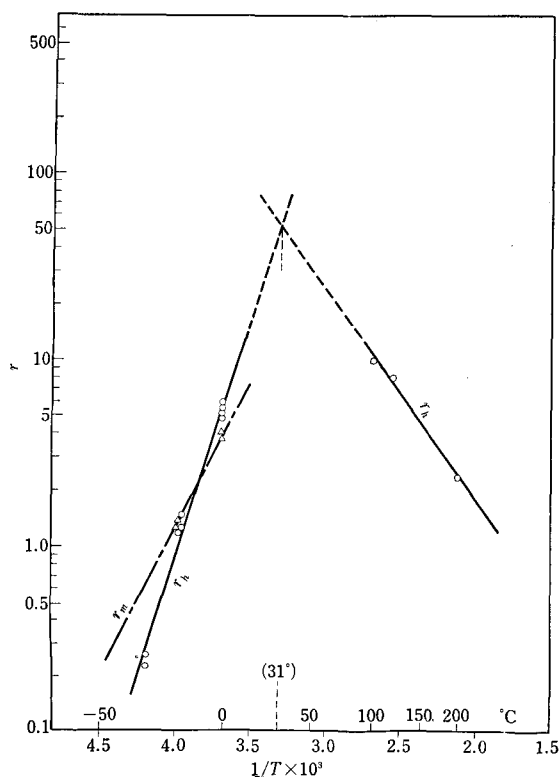


Fig. 9. Temperature dependence of reaction rate.

$$P_H^0 = 39-40 \text{ mmHg}, \quad P_N^0 = 34-35 \text{ mmHg}$$

The rate of hydrogenation increases rapidly with temperature between  $-30$  and  $0^{\circ}\text{C}$ , but decreases slowly above  $100^{\circ}\text{C}$  as shown in Fig. 9, the appropriate activation energies being  $11.8$  and  $-5.6$  Kcal/mol respectively. The optimum temperature is located on the intersection at  $31^{\circ}\text{C}$  of the two lines in Fig. 9. The activation energy of DBM was found to be  $7.2$  Kcal from the slope of the chain line in Fig. 9.

### § 8. Reaction at High Temperature

A trace of *iso*-butane was found in the product at high temperatures above  $120^{\circ}\text{C}$ , whereas no isomerization of carbon skelton was observed at temperatures below  $0^{\circ}\text{C}$ . The result obtained at  $198^{\circ}\text{C}$  is shown in Table 12 as an exmple.

The total pressure of hydrocarbons decreased by  $4.8\%$  through the reaction as shown in Table 12, which could not be attributed to the dissolution into grease according to § 3. This should be due to polymerization to higher

TABLE 12. Distribution of hydrocarbons in the product at 198°C.

catalyst: 0.023 g,  $P_0^H = 40.6$  mmHg, reaction time: 16.3 min

	Total pressure	$C_2H_4$	$C_2H_6$	$C_3H_6$	$C_3H_8$	<i>iso</i> - $C_4H_{10}$	<i>n</i> - $C_4H_{10}$	1- $C_4H_8$	<i>trans</i> -2- $C_4H_8$	<i>cis</i> -2- $C_4H_8$
Reactant	35.5	—	trace	0.10	0.10	—	0.9	89.5	4.5	4.9
Product	33.8	—	0.03	0.09	0.16	trace	12.4	7.4	8.6	5.1

hydrocarbons possibly accompanied or by cracking to lower hydrocarbons. The cracking took place actually as evidenced by the increase of total amount of  $C_2$  and  $C_3$  hydrocarbons through the reaction. Methane was not detectable, if formed at all, because it could not be condensed by liquid nitrogen trap. Neither the polymerization was ascertained because higher hydrocarbons than

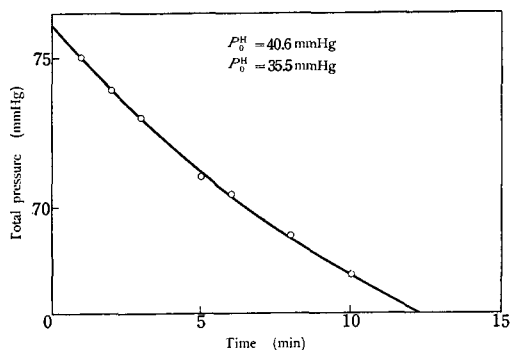


Fig. 10 (a). Decrease of total pressure with time at 198°C.

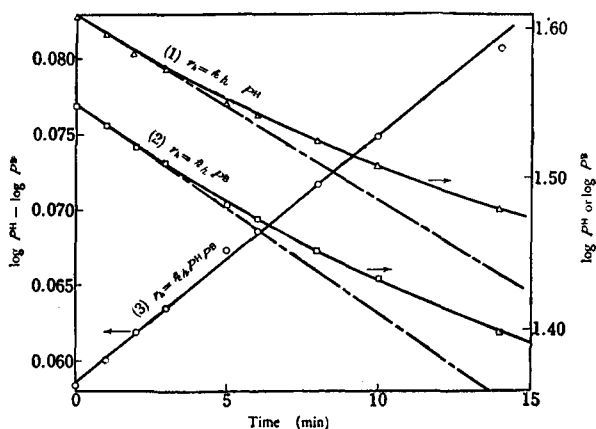


Fig. 10 (b). Fit of rate equations.

C<sub>4</sub> did not practically elute the gas chromatographic column.

Fig. 10 (a) shows the decrease of the total pressure with time. The order of reaction of hydrogenation was determined by fitting the above data severally to the rate equations (1), (2) and (3), *i. e.* (1)  $r_h = k_h P^H$ , (2)  $r_h = k_h P^B$ , (3)  $r_h = k_h P^H P^B$ , respectively integrated as (1)', (2)' and (3)', *i. e.* (1)'  $\log P^H = C_1 t - C_{01}$ , (2)'  $\log P^B = C_2 t - C_{02}$ , (3)'  $\log P^H - \log P^B = C_3 t - C_{03}$ , where  $k_h$ ,  $C_1$  etc. are constants,  $t$  the reaction time. The partial pressures were derived from the total pressure observed neglecting its decrease mentioned above. The left side of (1)', (2)' and (3)' were respectively worked out from the partial pressures thus obtained and plotted against time as shown in Fig. 10 (b). The Figure indicates distinctly that the rate law (3) is confirmed exclusively by the experiment, *i. e.* that the hydrogenation at the high temperature is of first order with respect both to hydrogen and butene.

As mentioned in §6 the content of 2-butenes in the product increases along with the progress of hydrogenation to approach the isomeric composition of butene in equilibrium. The compositions of the products at different temperatures are shown in Table 14, and the corresponding equilibrium compo-

TABLE 13. Equilibrium composition of *n*-butenes\*

Temperature (°C)	1-butene (%)	<i>trans</i> -2-butene (%)	<i>cis</i> -2-butene (%)	total 2-butenes (%)
0	2.0	78.4	19.6	98.0
100	4.5	66.2	29.3	95.5
198	9.0	59.5	31.5	91.0

\* Calculated from *Selected Values of Physical and Thermodynamic Properties of Hydrocarbons and Related Substances*. Rossini, Carnegie Press, 1953.

TABLE 14. Composition of butenes in product  
catalyst: 0.023 g,  $P_0^H$ : 39.7-41.1 mmHg,  $P_0^B$ : 34.7-35.5 mmHg

No. of Runs	Temperature (°C)	Hydrogen consumed (%)	1-butene (%)	<i>trans</i> -2- butene (%)	<i>cis</i> -2- butene (%)	total-2- butenes (%)	$\frac{(\text{total-2-butenes})^*}{(\text{total-2-butenes})_E}$ (%)
Reactant	—	—	90.3	4.5	5.2	9.7	—
269	0	35.8	83.4	9.4	7.2	16.6	9.9
268	100	31.6	78.2	12.4	9.4	21.8	22.8
279	198	29.8	35.2	40.5	24.3	64.8	71.2

\* (total 2-butenes)<sub>E</sub> expresses total 2-butenes in equilibrium at each reaction temperature, which was shown in the last column of Table 13.

sition at each temperature in Table 13. The notation (total-2-butenes)<sub>B</sub> in Table 14 represents the content of total 2-butenes in equilibrium, which is given in the last column of Table 13. Table 14 shows the content of 2-butenes approaches rapidly to that in equilibrium with rise of temperature, notwithstanding the smaller extent of hydrogenation at higher temperature than at lower temperature, *i. e.* that  $r_m$  increases with temperature more rapidly than  $r_h$  does.

The results obtained in the present experiment are summarized in Table 15.

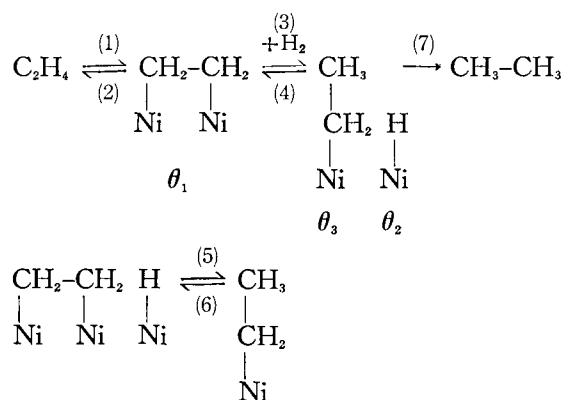
TABLE 15. Order of reaction and activation energy

		Low temp. (<0°C)	High temp. (>100°C)
Hydrogenation	{ Order of reaction	(PH) <sup>1</sup> (PB) <sup>0</sup>	(PH) <sup>1</sup> (PB) <sup>1</sup>
	{ Activation energy	11.8 Kcal	-5.6 Kcal
Isomerization 1-butene→2-butenes	{ Order of reaction	(PH) <sup>0.6</sup> (P <sup>1</sup> -B) <sup>0.5</sup>	
	{ Activation energy	7.2 Kcal	

### Chapter III. Discussion

#### § 9. TWIGG's Mechanism

TWIGG<sup>3)</sup> has proposed the following mechanism for the catalyzed hydrogenation of ethene in the presence of nickel catalyst:



This mechanism leads to the relations at the steady state

$$\theta_2 = \left[ \frac{k_3 k_6}{k_5 (k_4 + k_7)} P^{\text{H}} \right]^{\frac{1}{2}}$$

$$\theta_3 = \left[ \frac{k_3 k_5}{k_6 (k_4 + k_7)} P^{\text{H}} \right]^{\frac{1}{2}} \theta_1,$$

where  $\theta_1$ ,  $\theta_2$  and  $\theta_3$  are the surface concentration of adsorbed ethene, adsorbed hydrogen atom and adsorbed ethyl radical respectively,  $k_1$  etc. are the rate constants of steps (1) etc., and  $P^H$  the partial pressure of hydrogen. He tried to interpret his experimental results of the hydrogenation and DBM of 1-butene on the base of the reaction scheme corresponding to the above one of ethene. Assuming that the rate of DBM is the same as that corresponding to the step (6) in which adsorbed butyl radical dissociates into adsorbed butene and hydrogen atom and that  $\theta_1=1$  at low temperature, he derived the rates of hydrogenation and DBM in terms of the similar notations as

$$r_h = k_7\theta_2\theta_3 = \left(\frac{k_3k_7}{k_4+k_7}\right)P^H\theta_1 \doteq k_hP^H$$

$$r_m = k_8\theta_3 = \left(\frac{k_3k_5k_8}{k_4+k_7}\right)^{\frac{1}{2}}(P^H)^{\frac{1}{2}}\theta_1 = k_m(P^H)^{\frac{1}{2}},$$

where  $k_h$  and  $k_m$  were the rate constants of hydrogenation and DBM respectively. The rate law observed by TWIGG himself<sup>3)</sup> and DIBELER and TAYLOR<sup>4)</sup>, however, were such that  $r_h = k_h(P^H)^{\frac{1}{2}}(P^{1-B})^{\frac{1}{2}}$  and  $r_m = k_m(P^H)^{\frac{1}{2}}(P^{1-B})^{\frac{1}{2}}$ , which disagreed with the above theoretical conclusions.

The results obtained by the present author suggest on the contrary as shown in § 5, that the adsorption of butene was very weak even at 0°C over the pressure region used by TWIGG and DIBELER and TAYLOR, hence that  $\theta_1 = KP^{1-B}$  instead of  $\theta_1 = 1$ , where  $K$  is a constant. It follows that

$$r_h \doteq k_hP^HP^{1-B}$$

$$r_m \doteq k_m(P^H)^{\frac{1}{2}}P^{1-B}$$

which fits in neither with their result nor with that of the present author.

### § 10. HORIUTI and POLANYI's Mechanism

HORIUTI<sup>7)8)</sup> successfully explained ZUR STRASSEN's results<sup>9)</sup> on the base of the scheme of Fig. 11 (a) proposed by HORIUTI and POLANYI<sup>5)6)</sup>, by means of statistical mechanical analysis. The reaction scheme of butene may be formulated analogously to that of the ethene hydrogenation, as shown in Fig. 11 (b), where DBM occurs through the steps I<sub>a</sub> and II<sub>b</sub> forwards, and then II<sub>c</sub> and I<sub>a</sub> backwards. The present discussion will be simplified assuming that adsorbed 1-butene and adsorbed 2-butenes are created and consumed by the relevant steps with equal opportunity and the same is true with the other pair of isomeric intermediates, *i. e.* the primary and secondary butyl radicals, hence isomeric intermediates and steps concerned may be lumped together as shown in Fig. 11 (c).

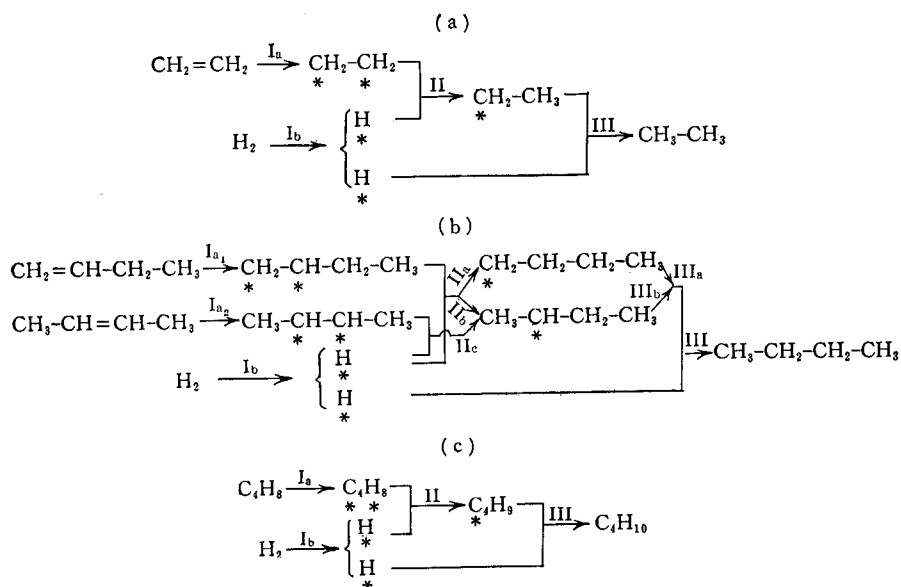


Fig. 11. Reaction schemes of hydrogenation of ethene and butene.

The scheme of Fig. 11 (c) is, however, formally identical with that of Fig. 11 (a) for ethene. On this basis the present experimental results will be analyzed in the following sections in accordance with the HORIUTI's method for ethene.

### § 11. Condition of Steady Reaction

The rate  $V_S$  of the steady reaction of Fig. 11 (c) is written as

$$V_S = \bar{v}(\text{I}_a) - \bar{v}(\text{I}_a) = \bar{v}(\text{I}_b) - \bar{v}(\text{I}_b) = \bar{v}(\text{II}) - \bar{v}(\text{II}) = \bar{v}(\text{III}) - \bar{v}(\text{III}), \quad (11.1)$$

where  $\bar{v}(S)$  and  $\bar{v}(S)$  are the forward and backward rates of the step  $S$  respectively. The rates  $\bar{v}(S)$  and  $\bar{v}(S)$  are given statistically mechanically as

$$\bar{v}(S) = \mathfrak{K}(S) \frac{p_e^{\text{I}(S)}}{p^{\text{I}(S)}}, \quad \bar{v}(S) = \mathfrak{K}(S) \frac{p_e^{\text{I}(S)}}{p^{\text{F}(S)}}, \quad (11.1)$$

where

$$\mathfrak{K}(S) = \frac{kT}{h} p^{*(S)} / p_e^{\text{I}(S)}, \quad (11.3)$$

$p^{\text{I}(S)}$ ,  $p^{\text{F}(S)}$  and  $p^{*(S)}$  are the BOLTZMANN factors of the chemical potential, of the initial, final and critical complex of the step  $S$  respectively,  $k$  or  $h$  the BOLTZMANN or the PLANCK constant and  $T$  the absolute temperature;  $p_e^{\text{I}(S)}$

and  $p_e^{F(S)}$  represent the particular values of  $p^{I(S)}$  and  $p^{F(S)}$  in the case, where every step but  $S$  is in equilibrium. It is obvious from (11.2) that  $\mathfrak{K}(S)$  represents the rate of the forward reaction of the step  $S$  in the particular case, where  $p^{I(S)} = p_e^{I(S)}$ .

Denoting hydrogen and butene in gas by H and B respectively,  $p_e^{I(S)}$  is written as

$$p_e^{I(I_a)} = p^B, \quad p_e^{I(I_b)} = p^H, \quad p_e^{I(II)} = (p^H)^{1/2} p^B, \quad p_e^{I(III)} = p^H p^B. \quad (11.4)$$

We introduce now the quantities  $\gamma(H)$ ,  $\gamma(C_4H_8)$ ,  $\gamma(C_4H_9)$  and  $\Gamma$  defined as

$$\left. \begin{aligned} \gamma(H) &= (p^H)^{1/2} / p^{H(a)}, & \gamma(C_4H_8) &= p^B / p^{C_4H_8(a)} \\ \gamma(C_4H_9) &= p^B (p^H)^{1/2} / p^{C_4H_9(a)}, & \Gamma &= p_e^{I(III)} / p^{F(III)} = p^B p^H / p \end{aligned} \right\} \quad (11.5)$$

where (a) denotes the adsorbed state and A butane in gas. The quantity  $\gamma(H)$ , for example, is the relative activity of H(a) referred to the absolute activity of H(a) at the particular state, where all steps in Fig. 11 (c) which derive H(a) from the reactant H+B are respectively in equilibrium.

The rates  $\bar{v}(S)$  and  $\tilde{v}(S)$  are expressed by (11.2), (11.4) and (11.5) as

$$\left. \begin{aligned} \bar{v}(I_a) &= \mathfrak{K}(I_a), & \tilde{v}(I_b) &= \mathfrak{K}(I_b), & \tilde{v}(II) &= \gamma(C_4H_8) \gamma(H) \mathfrak{K}(II) \\ \tilde{v}(III) &= \gamma(C_4H_9) \gamma(H) \mathfrak{K}(III) \\ \bar{v}(I_a) &= \gamma(C_4H_8) \mathfrak{K}(I_a), & \tilde{v}(I_b) &= \gamma(H)^2 \mathfrak{K}(I_b), & \tilde{v}(II) &= \gamma(C_4H_9) \mathfrak{K}(II) \\ \bar{v}(III) &= \Gamma \mathfrak{K}(III). \end{aligned} \right\} \quad (11.6)$$

Hence (11.1) is written as

$$\left. \begin{aligned} V_S &= \mathfrak{K}(I_a)(1 - \gamma(C_4H_8)) = \mathfrak{K}(I_b)(1 - \gamma(H)^2) \\ &= \mathfrak{K}(II)(\gamma(H)\gamma(C_4H_8) - \gamma(C_4H_9)) = \mathfrak{K}(III)(\gamma(H)\gamma(C_4H_9) - \Gamma). \end{aligned} \right\} \quad (11.7)$$

The factor  $p^{*(S)}$  is written for a step occurring on a surface as<sup>8)</sup>

$$p^{*(S)} = G^{*(S)} q^{*(S)} \theta_{\sigma_s^*}^{*(S)}. \quad (11.8)$$

where  $\theta_{\sigma_s^*}^{*(S)}$  is the probability of a site  $\sigma_s^*$  for the critical complex  $*(S)$  of the step  $S$  being unoccupied,  $G^{*(S)}$  the number of sites  $\sigma_s^*$  per unit area of the surface;  $q^{*(S)}$  is the BOLTZMANN factor of the reversible work  $\epsilon^{*(S)}$  *i.e.* that at statistical equilibrium required to bring up a critical complex  $*(S)$  from its standard state to set it up in a definite, preliminarily evacuated site  $\sigma_s^*$ , *i.e.*

$$q^{*(S)} = \exp(-\epsilon^{*(S)}/RT).$$

And  $p^H$  and  $p^B$  are expressed as<sup>8)</sup>

$$p^H = Q^H/N^H, \quad p^B = Q^B/N^B, \quad (11.9)$$

where  $Q^H$  and  $Q^B$  is the partition function of a single gaseous molecule in unit volume,  $N^H$  or  $N^B$  the concentration in gas of hydrogen or butene respectively.

Defining  $K_{N(S)}$  as

$$K_{N(S)} = \frac{kT}{h} G^{*(S)} q^{*(S)} \theta_{\sigma_S^{*(S)}}, \quad (11.10)$$

$\mathfrak{K}(S)$  is written by (11.3), (11.4), (11.8), (11.9) and (11.10) as

$$\left. \begin{aligned} \mathfrak{K}(I_a) &= K_N(I_a) N^B / Q^B, & \mathfrak{K}(I_b) &= K_N(I_b) N^H / Q^H \\ \mathfrak{K}(II) &= K_N(II) N^B (N^H)^{1/2} / Q^B (Q^H)^{1/2}, & \mathfrak{K}(III) &= K_N(III) N^B N^H / Q^B Q^H. \end{aligned} \right\} \quad (11.11)$$

We have on the other hand from (11.7)

$$\begin{aligned} V_S &= \frac{\gamma(H)^2 (1 - \gamma(C_4H_8))}{\gamma(H)^2 / \mathfrak{K}(I_a)} = \frac{1 - \gamma(H)^2}{1 / \mathfrak{K}(I_b)} = \frac{\gamma(H)^2 \gamma(C_4H_8) - \gamma(H) \gamma(C_4H_8)}{\gamma(H) / \mathfrak{K}(II)} \\ &= \frac{\gamma(H) \gamma(C_4H_8) - \Gamma}{1 / \mathfrak{K}(III)} = \frac{1 - \Gamma}{\gamma(H)^2 / \mathfrak{K}(I_a) + 1 / \mathfrak{K}(I_b) + \gamma(H) / \mathfrak{K}(II) + 1 / \mathfrak{K}(III)}, \end{aligned} \quad (11.12)$$

hence

$$\frac{1 - \Gamma}{V_S} = \frac{\gamma(H)^2}{\mathfrak{K}(I_a)} + \frac{1}{\mathfrak{K}(I_b)} + \frac{\gamma(H)}{\mathfrak{K}(II)} + \frac{1}{\mathfrak{K}(III)}, \quad (11.13)$$

or

$$\frac{1 - \Gamma}{V_S} = \frac{\gamma(H)^2 Q^B}{K_N(I_a) N^B} + \frac{Q^H}{K_N(I_b) N^H} + \frac{\gamma(H) (Q^H)^{1/2} Q^B}{K_N(II) (N^H)^{1/2} N^B} + \frac{Q^H Q^B}{K_N(III) N^H N^B}, \quad (11.14)$$

according to (11.11).

## § 12. Rate-Determining Step

The quantity  $\Gamma$  is given according to (11.5) and (11.9) as<sup>8)</sup>

$$\Gamma = \frac{P^A}{P^H P^B} \cdot \frac{1}{K_P}$$

where  $P^H$ ,  $P^B$  and  $P^A$  are the partial pressures of hydrogen, butene and butane respectively under the condition of the experiment,  $K_P$  the equilibrium constant expressed by pressure. Table 16 shows the values of  $\Gamma$  calculated by the above equation for the condition  $P^A = P^H = P^B = 10$  mmHg. It is obvious that  $\Gamma$  is negligibly smaller than unity, although positive by definition, *i. e.*

$$0 < \Gamma \ll 1 \quad (12.1)$$

TABLE 16.  $\Gamma$   
 $P^A = P^H = P^B = 10$  mmHg

Temperature °K	298.16	300	400	500
$K_P^*$	$3.40 \times 10^{15}$	$2.47 \times 10^{15}$	$9.80 \times 10^9$	$3.64 \times 10^6$
$\Gamma$	$2.94 \times 10^{-17}$	$4.05 \times 10^{-17}$	$1.02 \times 10^{-11}$	$2.75 \times 10^{-8}$

\*  $K_P$  was calculated from *Selected Values of Physical and Thermodynamic Properties of Hydrocarbons and Related Substances*. Rossini, Carnegie Press, 1953.

It follows, on the other hand, from (11.7) and (12.1) along a line of reasoning formally identical with that in the case of ethene hydrogenation<sup>9)</sup>, that

$$V_s > 0, \quad 1 > \gamma(\text{C}_4\text{H}_8), \quad \gamma(\text{H}), \quad \gamma(\text{C}_4\text{H}_8) > 0, \quad (12.2)$$

$$V_s/(1-\Gamma) < \mathfrak{K}(S), \quad S = \text{I}_a, \text{I}_b, \text{II}, \text{III}, \quad (12.3)$$

$$V_s/(1-\Gamma) \text{ approaches } \mathfrak{K}(r), \text{ as } \mathfrak{K}(r) \text{ grows less than all other } \mathfrak{K}(S) \quad (12.4. a)$$

and conversely that

$$\mathfrak{K}(S) \text{ of step } S \text{ other than } r \text{ grows infinitely larger than } \mathfrak{K}(r), \text{ as } \mathfrak{K}(r) \text{, approaches } V_s/(1-\Gamma). \quad (12.4. b)$$

Step  $r$  will be called the rate-determining step, as  $\mathfrak{K}(r)$  is sufficiently small compared with all other  $\mathfrak{K}(S)$ .

The rate-determining step  $r$  is now decided on the basis of the experimental data in what follows.

We have from the equation of the first and third members of (11.7) and the second equation of (11.11)

$$V_s/N^H = K(\text{I}_b)(1-\gamma(\text{H})^2)/Q^H \quad (12.5)$$

Assuming that the surface of catalyst is practically bare under the butene pressure below 120 mmHg as suggested by the experimental results of § 5, both  $G^{*(S)}\theta_{s(S)}^*$  and  $q^{*(S)}$  may be taken constant at constant temperature. It follows from (11.10) that  $K_N(S)$  is constant irrespective of partial pressures in gas phase. The present experiment shows, on the other hand, that the rate  $V_s$  was proportional to the partial pressure of hydrogen or to  $N^H$  both over the regions of lower and higher temperatures. The left side  $V_s/N^H$  of (12.5) should hence be constant at constant  $N^B$  independent of  $N^H$ . Therefore,  $\gamma(\text{H})^2$  on the right side of (12.5) must be either constant independent of the partial pressure of hydrogen, or far smaller than unity.

First consider the case that  $\gamma(\text{H})$  is constant. Multiplying the both sides of (11.14) by  $N^{\text{H}}$ , we have

$$\frac{N^{\text{H}}(1-\Gamma)}{V_s} := \frac{\gamma(\text{H})^2 Q^{\text{B}} N^{\text{H}}}{K_N(\text{I}_a) N^{\text{B}}} + \frac{Q^{\text{H}}}{K_N(\text{I}_b)} + \frac{\gamma(\text{H})(Q^{\text{H}})^{1/2} Q^{\text{B}} (N^{\text{H}})^{1/2}}{K_N(\text{II}) N^{\text{B}}} + \frac{Q^{\text{H}} Q^{\text{B}}}{K_N(\text{III}) N^{\text{B}}}. \quad (12.6)$$

The left side  $N^{\text{H}}(1-\Gamma)/V_s$  of the above equation is practically constant independent of hydrogen pressure according to (12.1). Therefore, the first and third terms on the right side of (12.6), which depend on  $N^{\text{H}}$  must be negligibly small compared with the other terms, *i. e.*

$$\frac{1}{V_s} := \frac{Q^{\text{H}}}{K_N(\text{I}_b) N^{\text{H}}} + \frac{Q^{\text{H}} Q^{\text{B}}}{K_N(\text{III}) N^{\text{H}} N^{\text{B}}}, \quad (12.7)$$

or by (11.11)

$$\frac{1}{V_s} = \frac{1}{\mathfrak{K}(\text{I}_b)} + \frac{1}{\mathfrak{K}(\text{III})}. \quad (12.8)$$

As  $V_s$  is independent of  $N^{\text{B}}$  at low temperature, the second term on the right side of (12.7) or (12.8) must be practically negligible there, *i. e.*

$$V_s = \mathfrak{K}(\text{I}_b). \quad (12.9)$$

If  $\gamma(\text{H})^2 \ll 1$ , the same equation as (12.9) is derived from (11.7). It follows from (12.4 b) and (12.9) that  $\text{I}_b$  is the rate-determining step at lower temperature.

At higher temperature, where  $V_s$  is proportional to  $N^{\text{H}} N^{\text{B}}$ , the first term on the right side of (12.7) or (12.8) must practically vanish, *i. e.* as

$$V_s = \mathfrak{K}(\text{III}). \quad (12.10)$$

The rate-determining step is III at higher temperature as deduced from (12.10) and (12.4. b).

### § 13. $\gamma(\text{C}_4\text{H}_8)$

The quantity  $\gamma(\text{C}_4\text{H}_8)$  will be determined for the case that  $V_s \doteq \mathfrak{K}(\text{I}_b)$  at lower temperature.

It follows from (12.4. b), (12.9) and (12.10) with reference to (12.1) that  $\mathfrak{K}(\text{I}_a) \gg V_s$  both at lower and higher temperature, hence from the equation of the first and second members of (11.7), that

$$\gamma(\text{C}_4\text{H}_8) \doteq 1 \quad (13.1)$$

Equation (11.7) reduces now to the form

$$V_s = \mathfrak{K}(\text{I}_b) = \mathfrak{K}(\text{II})(\gamma(\text{H}) - \gamma(\text{C}_4\text{H}_8)) = \mathfrak{K}(\text{III})(\gamma(\text{H})\gamma(\text{C}_4\text{H}_8) - \Gamma). \quad (13.2)$$

We have from (13.2),

$$\mathfrak{R}(\text{I}_b)/\mathfrak{R}(\text{II}) = \gamma(\text{H}) - \gamma(\text{C}_4\text{H}_9), \quad (13.3)$$

$$\mathfrak{R}(\text{I}_b)/\mathfrak{R}(\text{III}) = \gamma(\text{H}) \cdot \gamma(\text{C}_4\text{H}_9) - \Gamma, \quad (13.4)$$

which is solved for  $\gamma(\text{C}_4\text{H}_9)$  as

$$\gamma(\text{C}_4\text{H}_9) = \frac{\mathfrak{R}(\text{I}_b)}{2\mathfrak{R}(\text{II})} \left\{ -1 + \sqrt{1 + 4 \frac{\mathfrak{R}(\text{II})^2}{\mathfrak{R}(\text{I}_b)\mathfrak{R}(\text{III})} \left( 1 + \Gamma \frac{\mathfrak{R}(\text{III})}{\mathfrak{R}(\text{I}_b)} \right)} \right\}. \quad (13.5)$$

Ignoring  $\Gamma\mathfrak{R}(\text{III})/\mathfrak{R}(\text{I}_b)$  compared with unity<sup>\*)</sup>, we have

$$\gamma(\text{C}_4\text{H}_9) = \frac{\mathfrak{R}(\text{I}_b)}{2\mathfrak{R}(\text{II})} \left\{ -1 + \sqrt{1 + 4 \frac{\mathfrak{R}(\text{II})^2}{\mathfrak{R}(\text{I}_b)\mathfrak{R}(\text{III})}} \right\}, \quad (13.6)$$

#### § 14. $r_m$

Let  $\bar{v}(\text{II}_i)$  and  $\bar{v}(\text{II}_i)$  be the forward and backward rates of  $\text{II}_i$ , where  $i = a, b, c$ , as indicated in Fig. 11 (b). The rates  $\bar{v}(\text{II})$  or  $\bar{v}(\text{II})$  is the overall rate of formation both of primary and secondary butyl radicals from adsorbed 1- and 2-butenes or its reversal respectively as seen from the comparison of (b) and (c) of Fig. 11, so that we have

$$\left. \begin{aligned} \bar{v}(\text{II}_a) + \bar{v}(\text{II}_b) + \bar{v}(\text{II}_c) &= \bar{v}(\text{II}) \\ \bar{v}(\text{II}_a) + \bar{v}(\text{II}_b) + \bar{v}(\text{II}_c) &= \bar{v}(\text{II}) \end{aligned} \right\} \quad (14.1)$$

We have in accordance with §10

$$\left. \begin{aligned} \bar{v}(\text{II}_a) &= \bar{v}(\text{II}_b) = \frac{1}{2} \bar{v}(\text{II})x \\ \bar{v}(\text{II}_c) &= \bar{v}(\text{II})(1-x), \end{aligned} \right\} \quad (14.2)$$

and

$$\left. \begin{aligned} \bar{v}(\text{II}_a) &= \bar{v}(\text{II})yC \\ \bar{v}(\text{II}_b) &= \bar{v}(\text{II}_c) = \bar{v}(\text{II})(1-y)C, \end{aligned} \right\} \quad (14.3)$$

where  $x$  is the mole fraction of adsorbed 1-butene in total adsorbed butenes,  $y$  is the mole fraction of primary butyl radical in total butyl radicals, and  $C$  a constant, which is determined from (14.1) and (14.3) as

$$C = \frac{1}{2-y}$$

hence

\*) It is shown in §15 that  $\Gamma\mathfrak{R}(\text{III})/\mathfrak{R}(\text{I}_b)$  is extremely small compared with unity.

$$\left. \begin{aligned} \bar{v}(\text{II}_a) &= \bar{v}(\text{II}) \frac{y}{2-y} \\ \bar{v}(\text{II}_b) &= \bar{v}(\text{II}_c) = \bar{v}(\text{II}) \frac{1-y}{2-y} \end{aligned} \right\} \quad (14.4)$$

Similarly we have

$$\left. \begin{aligned} \bar{v}(\text{III}_a) &= \bar{v}(\text{III})y, \\ \bar{v}(\text{III}_b) &= \bar{v}(\text{III})(1-y), \end{aligned} \right\} \quad (14.5)$$

where  $\bar{v}(\text{III}_a)$  and  $\bar{v}(\text{III}_b)$  are the forward rates of  $\text{III}_a$  and  $\text{III}_b$  indicated in Fig. 11 (b).

The conditions of steady reaction are now stated with respect to secondary butyl radical and overall butyl radical, ignoring  $\bar{v}(\text{III})$ , which is extremely small as compared with  $\bar{v}(\text{II})$  or  $\bar{v}(\text{II})$  as shown in § 16, as

$$\bar{v}(\text{II}_b) - \bar{v}(\text{II}_b) + \bar{v}(\text{II}_c) - \bar{v}(\text{II}_c) - (1-y)\bar{v}(\text{III}) = 0, \quad (14.6)$$

$$\bar{v}(\text{II}) - \bar{v}(\text{II}) = \bar{v}(\text{III}). \quad (14.7)$$

We have from (14.2), (14.4) and the above equations,

$$\bar{v}(\text{II}) \left( \frac{x}{2} - y \right) - \bar{v}(\text{II}) \frac{y(y-1)}{2-y} = 0. \quad (14.8)$$

The same conclusion is arrived at from the steady condition with respect to primary butyl radical.

The rate  $r_m$  is now that of the unidirectional formation of 2-butenes from 1-butene through  $\text{II}_b$  and  $\text{II}_c$  minus the rate of its reversal. The former unidirectional rate is given by apportioning the rate  $\bar{v}(\text{II}_b)$  of the unidirectional supply of secondary butyl radical from 1-butene to the reverse rate of  $\text{II}_c$  by multiplying  $\bar{v}(\text{II}_b)$  by the fraction of  $\bar{v}(\text{II}_c)$  over the total rate  $\bar{v}(\text{II}_b) - \bar{v}(\text{II}_c) - (1-y)\bar{v}(\text{III})$  of the consumption of secondary butyl radical. Formulating the latter unidirectional rate similarly, we have

$$r_m = \bar{v}(\text{II}_b) \frac{\bar{v}(\text{II}_c)}{\bar{v}(\text{II}_b) + \bar{v}(\text{II}_c) + (1-y)\bar{v}(\text{III})} - \bar{v}(\text{II}_c) \frac{\bar{v}(\text{II}_b)}{\bar{v}(\text{II}_b) + \bar{v}(\text{II}_c) + (1-y)\bar{v}(\text{III})},$$

or eliminating  $\bar{v}(\text{II}_a)$ ,  $\bar{v}(\text{II}_c)$  and  $\bar{v}(\text{III})$  from (14.2), (14.4), (14.7) and the above equation,

$$r_m = \frac{\bar{v}(\text{II}) \bar{v}(\text{II}) \left( \frac{3}{2}x - 1 \right)}{\bar{v}(\text{II})(2-y) + \bar{v}(\text{II})y}. \quad (14.9)$$

The rate  $r_m$  is now expressed in terms of  $\mathfrak{K}(S)$  to deduce the order of

reaction of DBM. The rate  $\bar{v}(\text{II})$  is given at lower temperature; where  $I_b$  determines the rate, according to (11.6) and (13.6), as

$$\bar{v}(\text{II}) = \frac{\mathfrak{K}(\text{I}_b)}{2}(-1 + \sqrt{1 + 4\kappa^2}), \quad (14.10. a)$$

where

$$\kappa^2 \equiv \mathfrak{K}(\text{II})^2 / \mathfrak{K}(\text{I}_b) \mathfrak{K}(\text{III}). \quad (14.10. b)$$

The rate  $r_m$  must, however, be smaller than  $\bar{v}(\text{II})^*$ , while  $\mathfrak{K}(\text{I}_b) = r_h$  by (12.9) at the specified condition. It follows that

$$\frac{2r_m}{r_h} < -1 + \sqrt{1 + 4\kappa^2}. \quad (14.11)$$

As the right side of (14.11) increases monotonously with  $\kappa$ ,  $4\kappa^2$  is necessarily larger than  $4\kappa_L^2$  which satisfy the equation

$$\frac{2r_m}{r_h} = -1 + \sqrt{1 + 4\kappa_L^2}.$$

Table 17 shows the numeral value of  $4\kappa_L^2$  which is calculated from the observed values of  $r_m$  and  $r_h$  in Tables 8 and 9.

Since  $4\kappa_L^2$  is about 26 at least, as shown in Table 17,  $4\kappa^2$  is larger than 26. Neglecting on this ground both the unities on the right side of (14.10. a),

TABLE 17.  $4\kappa_L^2$

Initial hydrogen pressure $P_0^{\text{H}}$ (mmHg)	Initial 1-butene pressure $P_0^{\text{1-B}}$ (mmHg)	$4\kappa_L^2$
24.5	23.4	25.73
24.8	41.8	39.96
24.7	64.5	63.96
25.1	92.3	86.42
10.4	99.9	126.7
25.1	100.0	87.36
37.8	100.0	52.58
63.3	100.7	45.79

\*) Equation (14.9) is written as

$$r_m = \left(\frac{3}{2}x - 1\right) \frac{\bar{v}(\text{II})}{\bar{v}(\text{II}) + \bar{v}(\text{II})(1-y) + \bar{v}(\text{II})y} \bar{v}(\text{II}).$$

The first and second factors on the right side of the above equation are both smaller than unity, because  $x \leq 1$  and  $y \leq 1$ , hence  $r_m < \bar{v}(\text{II})$ .

we have approximately\*)

$$\bar{v}(\text{II}) \doteq \mathfrak{K}(\text{II}) \sqrt{\mathfrak{K}(\text{I}_b)/\mathfrak{K}(\text{III})}, \quad (14.12)$$

and from (13.6) similarly

$$\gamma(\text{C}_4\text{H}_8) = \sqrt{\mathfrak{K}(\text{I}_b)/\mathfrak{K}(\text{III})}. \quad (14.13)$$

The quantity  $\gamma(\text{H})$  is given by (13.4) and the above equation, neglecting  $I$ , as

$$\gamma(\text{H}) = \sqrt{\mathfrak{K}(\text{I}_b)/\mathfrak{K}(\text{III})}. \quad (14.14)$$

It follows from (11.6), (13.1) and the above two equations, that

$$\bar{v}(\text{II}) = \bar{v}(\text{II}). \quad (14.15)$$

Equation (14.9) is hence simplified by the above equation as

$$r_m = \left( \frac{3}{4}x - \frac{1}{2} \right) \bar{v}(\text{II}), \quad (14.16)$$

which states that  $r_m$  is proportional to  $\bar{v}(\text{II})$ , hence that the order of reaction of DBM is the same as that of the reversal of II. There exist, on the other hand, the following relations according to (11.11):

$$\mathfrak{K}(\text{I}_b) \propto P^{\text{H}}, \quad \mathfrak{K}(\text{II}) \propto (P^{\text{H}})^{\frac{1}{2}}(P^{1-\text{B}}), \quad \mathfrak{K}(\text{III}) \propto P^{\text{H}}P^{1-\text{B}}. \quad (14.17)$$

Hence we have from (14.12) and (14.16)

$$r_m \propto \bar{v}(\text{II}) \propto (P^{\text{H}})^{0.5}(P^{1-\text{B}})^{0.5}, \quad (14.18)$$

which agrees excellently with the experimental result (6.3). The order of reaction is just insignificantly changed as shown in Appendix, if deduced without the above approximation which leads to (14.16).

## § 15. Structure of Hydrogenation

HORIUTI determined the so-called structure of the hydrogenation of ethene which accounted for various experimental results, by evaluating  $\mathfrak{K}(\text{I}_b)$ ,  $\mathfrak{K}(\text{II})$  and  $\mathfrak{K}(\text{III})$  statistical mechanically<sup>7)8)</sup>. This method will be applied to deduce the structure of hydrogenation of 1-butene on the basis of the scheme of Fig. 11 (c).

The rate  $\mathfrak{K}(S)$  is expressed statistical mechanically as

$$\mathfrak{K}(\text{I}_b)/\rho = (\mathfrak{K}(\text{I}_b)_\infty/\rho) \exp(-\Delta^*\varepsilon(\text{I}_b)/RT), \quad (15.1. \text{I}_b)$$

$$\mathfrak{K}(\text{II})/\rho = (\mathfrak{K}(\text{II})_\infty/\rho) \exp(-\Delta^*\varepsilon(\text{II})/RT), \quad (15.1. \text{II})$$

$$\mathfrak{K}(\text{III})/\rho = (\mathfrak{K}(\text{III})_\infty/\rho) \exp(-\Delta^*\varepsilon(\text{III})/RT), \quad (15.1. \text{III})$$

\*) Determination of the order of reaction of DBM without this approximation will be given in Appendix.

where

$$\mathfrak{K}(\text{I}_b)_\infty/\rho = P^{\text{H}}/Q_P^{\text{H}}, \quad (15.2. \text{I}_b)$$

$$\mathfrak{K}(\text{II})_\infty/\rho = P^{\text{B}}(P^{\text{H}})^{\frac{1}{2}}/Q_P^{\text{B}}(Q_P^{\text{H}})^{\frac{1}{2}}, \quad (15.2. \text{II})$$

$$\mathfrak{K}(\text{III})_\infty/\rho = P^{\text{B}}P^{\text{H}}/Q_P^{\text{B}}Q_P^{\text{H}}, \quad (15.2. \text{III})$$

and  $\rho = \frac{kT_N}{h} eG^{*(S)} \theta_{\sigma_S^*(c)}$  is a constant common to all  $\mathfrak{K}(S)$  at least in order of magnitude, provided that the catalyst surface is not very heavily covered;  $T_N$  is the average temperature over the temperature range in question, which is taken as 373°K in the present treatment;  $\Delta^* \varepsilon(S)$  is the activation energy of the elementary reaction  $S$  or the excess of the partial molal enthalpy of the critical complex of  $S$  over that of the set of molecules of the reactants, which is transformed into the initial complex of  $S$  through steps other than the step  $S$  in question, *i. e.* B for I<sub>b</sub>, B+1/2·H for II and B+H for III, where B or H denotes a butene or hydrogen molecule in gas;  $P^{\text{H}}$  and  $P^{\text{B}}$  are the partial pressures of hydrogen and 1-butene in mmHg respectively.  $Q_P^{\text{H}}$  and  $Q_P^{\text{B}}$  are the partition functions  $Q^{\text{H}}$  and  $Q^{\text{B}}$  in (11.9) transcribed as

$$Q_P^{\text{B}} = \frac{\kappa T_N}{1333} \frac{(2\pi m^{\text{B}} \kappa T_N)^{3/2}}{h^3} \frac{8\pi^2 (2\pi I^{\text{B}} \kappa T_N)^{3/2}}{h^3} e^{\Delta^* \varepsilon}, \quad (15.8. \text{B})$$

$$Q_P^{\text{H}} = \frac{\kappa T_N}{1333} \frac{(2\pi m^{\text{H}} \kappa T_N)^{3/2}}{h^3} \frac{4\pi^2 I^{\text{H}} \kappa T_N}{h^2} e^{\Delta^* \varepsilon}, \quad (15.8. \text{H})$$

so that  $P^{\text{H}}$  and  $P^{\text{B}}$  defined by (11.9) are invariantly expressed as  $P^{\text{B}}/Q_P^{\text{B}}$  and  $P^{\text{H}}/Q_P^{\text{H}}$  in the neighbourhood of  $T=T_N$ , where  $m^{\text{B}}$  or  $m^{\text{H}}$  is the mass of respective molecule,  $I^{\text{B}}$  the geometric mean of three principal moments of inertia of 1-butene,  $I^{\text{H}}$  the moment of inertia of hydrogen; the vibrational partition function was taken as unity both in the cases of 1-butene and hydrogen on the ground that the smallest vibrational wave number involved<sup>(11)</sup> is 400 cm<sup>-1</sup>. Transcribed partition function  $Q_P^{\text{B}}$  and  $Q_P^{\text{H}}$  calculated by the above equations are shown in Table 18 in comparison with that of ethene given by HORIUTI<sup>(8)</sup>.

TABLE 18.  $Q_P^{\text{H}}$ ,  $Q_P^{\text{E}}$ ,  $Q_P^{\text{B}}$  (E: Ethene)  
 $T_N=373^\circ\text{K}$

	Hydrogen	Ethene	1-Butene
$m$	$3.347 \times 10^{-24}$	$4.659 \times 10^{-23}$	$9.319 \times 10^{-23}$
$I_A I_B I_C$	$0.466 \times 10^{-40}$	$5.467 \times 10^{-117}$	$1.53 \times 10^{-114}$
$Q_P^{\text{H}}, Q_P^{\text{E}}, Q_P^{\text{B}}$	$1.057 \times 10^{10}$	$3.939 \times 10^{14}$	$7.461 \times 10^{16}$

TABLE 19.  $\log \mathfrak{K}(S)_\infty/\rho$   
 $P^{\text{H}}=40 \text{ mmHg}; P^{\text{B}}=35 \text{ mmHg}$

$S$	$\log \mathfrak{K}(S)_\infty/\rho$
I <sub>b</sub>	- 8.422
II	-19.540
III	-23.751

Table 19 shows the value of  $\log \hat{\mathfrak{R}}(S)_{\infty}/\rho$  calculated by (15.2) for the condition of the experiment described in §7 on the basis of the values of  $Q_p^B$  and  $Q_p^H$  in Table 18.

The structure of the hydrogenation was constructed as follows:  $\log \hat{\mathfrak{R}}(I_b)/\rho$  was first plotted against  $1/T$  in Fig. 12 with the value of  $\log \hat{\mathfrak{R}}(I_b)_{\infty}/\rho$  in Table 19 and the observed value  $\Delta^*_{\epsilon}(I_b)=11.8$  Kcal.

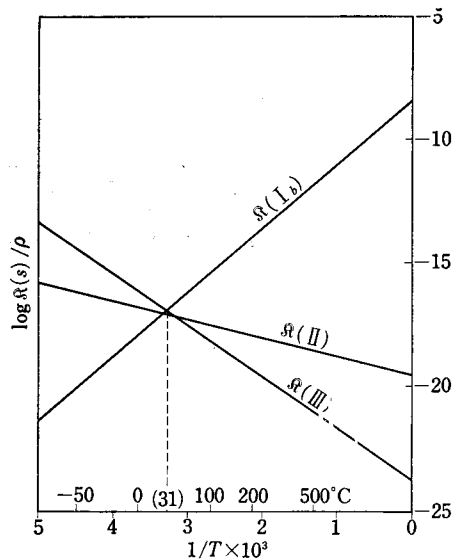


Fig. 12.  $\log \hat{\mathfrak{R}}(S)/\rho \sim 1/T$ .

The steady rate  $V_s$  of hydrogenation must now coincide with  $\hat{\mathfrak{R}}(I_b)$  and  $\hat{\mathfrak{R}}(III)$  at lower and higher temperature respectively in accordance with (12.9) and (12.10), hence  $\hat{\mathfrak{R}}(I_b)$ - and  $\hat{\mathfrak{R}}(III)$ - lines, which inclination differ in sign when plotted against  $1/T$ , should intersect approximately at the optimum temperature, which was located at 31°C in the present experiment. On this ground  $\hat{\mathfrak{R}}(III)$ -line in Fig. 12 was drawn by connecting the point at 31°C on  $\hat{\mathfrak{R}}(I_b)$ -line with the point of  $\log \hat{\mathfrak{R}}(III)_{\infty}/\rho$  by a straight line. The activation energy  $\Delta^*_{\epsilon}(III)$  was thus found to be  $-9.5$  Kcal from the slope of this line, which differed from the observed activation energy  $-5.6$  Kcal at higher temperature.

This difference may be due to the rapid flow of reactant gas at room temperature into the reactor at high temperature, which would lower the temperature of the catalyst from that of the thermostat\*) the more, the higher is the latter temperature, hence gives rise to too small an absolute value of the activation energy. On this ground, the value  $-9.5$  Kcal of  $\Delta^*_{\epsilon}(III)$  will be used in the following discussion.

The activation energy,  $\Delta^*_{\epsilon}(m)$  of DBM is expressed according to (14.16), (14.12), and (15.1) as

$$\Delta^*_{\epsilon}(m) = \Delta^*_{\epsilon}(II) + \frac{1}{2} \Delta^*_{\epsilon}(I_b) - \frac{1}{2} \Delta^*_{\epsilon}(III). \quad (15.4)$$

Hence, the activation energy  $\Delta^*_{\epsilon}(II)$  is calculated at  $-3.5$  Kcal from the observed values of  $\Delta^*_{\epsilon}(m)=7.2$  Kcal and  $\Delta^*_{\epsilon}(I_b)=11.8$  Kcal, and  $\Delta^*_{\epsilon}(III)=-9.5$  Kcal determined above. The  $\hat{\mathfrak{R}}(II)$ -line was constructed as in Fig. 12 on the base of this value of  $\Delta^*_{\epsilon}(II)$  and of  $\log \hat{\mathfrak{R}}(II)_{\infty}/\rho$  given in Table 19.

\*) Cf. § 3.

It is now shown that the condition  $F\mathfrak{K}(\text{III}) < \mathfrak{K}(\text{I}_b) \ll 1$  assumed with regard to (13.6) holds on the basis of the structure constructed above. Table 20 shows the value of  $\mathfrak{K}(\text{III})/\mathfrak{K}(\text{I}_b)$  calculated by (15.1) from the value of  $\log \mathfrak{K}(S)_\infty/\rho$  in Table 19, hence that  $F\mathfrak{K}(\text{III})/\mathfrak{K}(\text{I}_b)$  is smaller than  $10^{-11}$ , inasmuch as  $F$  is  $2.94 \times 10^{-17}$  at  $25^\circ\text{C}$  and smaller at lower temperature as reviewed in §12.

TABLE 20.  $\mathfrak{K}(\text{III})/\mathfrak{K}(\text{I}_b)$

Temperature	$\mathfrak{K}(\text{III})/\mathfrak{K}(\text{I}_b)$
$0^\circ\text{C}$	$5.27 \times 10^{-1}$
$-50$	$4.17 \times 10^5$

### § 16. Determination of $V_s$ , $r(\text{H})$ , $r(\text{C}_4\text{H}_9)$

The steady rate  $V_s$ ,  $r(\text{H})$  and  $r(\text{C}_4\text{H}_9)$  are derived from the structure just determined as follows. Equation (11.7) is written, according to (13.1), as

$$V_s = \mathfrak{K}(\text{I}_b)(1 - r(\text{H})^2) = \mathfrak{K}(\text{II})(r(\text{H}) - r(\text{C}_4\text{H}_9)) = \mathfrak{K}(\text{III})(r(\text{C}_4\text{H}_9) \cdot r(\text{H}) - F). \quad (16.1)$$

Neglecting  $F$  as compared with unity by (12.1), we have from the above equation

$$V_s = \frac{1}{\frac{1}{\mathfrak{K}(\text{I}_b)} + \frac{r(\text{H})}{\mathfrak{K}(\text{II})} + \frac{1}{\mathfrak{K}(\text{III})}}. \quad (16.2)$$

The values of  $V_s$  and  $r(\text{H})$  are determined by (16.2) and the equation  $V_s = \mathfrak{K}(\text{I}_b)(1 - r(\text{H})^2)$  of the first and the second members of (16.1) from the values of  $\mathfrak{K}(S)$  calculated as in the foregoing section.

The value of  $r(\text{C}_4\text{H}_9)$  is now determined by the equation of the second and last members of (16.1), *i. e.*

$$r(\text{C}_4\text{H}_9) = \frac{\mathfrak{K}(\text{I}_b)}{\mathfrak{K}(\text{III})} \cdot \frac{1 - r(\text{H})^2}{r(\text{H})} + \frac{F}{r(\text{H})}, \quad (16.3)$$

from the value of  $r(\text{H})$  determined above.

The rates  $\bar{v}(\text{II})$  and  $\bar{v}(\text{III})$  are expressed by (11.6) and (13.1) as

$$\bar{v}(\text{II}) = \mathfrak{K}(\text{II})r(\text{H}), \quad \bar{v}(\text{III}) = \mathfrak{K}(\text{III})r(\text{C}_4\text{H}_9), \quad (16.4)$$

by which their values are calculated as shown in Table 21 and Fig. 13 for the present experimental condition  $P^{\text{H}} = 40$  mmHg,  $P^{\text{B}} = 35$  mmHg of hydrogenation. The Table shows also that  $\bar{v}(\text{III})$  calculated by (11.6) is extremely small as compared with  $\bar{v}(\text{II})$  and  $\bar{v}(\text{I})$ .

As shown in Fig. 13, the steady rate  $V_s$  lies, on the structure diagram,

TABLE 21.  $V_S$ ,  $r(H)$ ,  $r(C_4H_9)$ ,  $\bar{v}(II)$ ,  $\bar{v}(II)$ ,  $\bar{v}(III)$ ,  $r_m$   
 $P^H = 40$  mmHg,  $P^B = 35$  mmHg

$t^\circ C$ $T^\circ K$	- 23 250	0 273	27 300	57 330	87 360
$\mathcal{R}(I_b)/\rho$	$1.738 \times 10^{-19}$	$1.356 \times 10^{-18}$	$9.623 \times 10^{-18}$	$5.816 \times 10^{-17}$	$2.344 \times 10^{-16}$
$\mathcal{R}(II)/\rho$	$3.162 \times 10^{-17}$	$1.828 \times 10^{-17}$	$1.022 \times 10^{-17}$	$5.995 \times 10^{-18}$	$3.802 \times 10^{-18}$
$\mathcal{R}(III)/\rho$	$3.715 \times 10^{-16}$	$7.143 \times 10^{-16}$	$1.475 \times 10^{-17}$	$3.465 \times 10^{-18}$	$1.023 \times 10^{-18}$
$V_S/\rho$	$1.737 \times 10^{-19}$	$1.315 \times 10^{-18}$	$4.070 \times 10^{-18}$	$2.130 \times 10^{-18}$	$8.040 \times 10^{-19}$
$r(H)$	0.02340	0.1710	0.7600	0.9815	0.9983
$r(C_4H_9)$	0.01998	0.1067	0.3626	0.6274	0.7802
$\bar{v}(II)/\rho$	$7.399 \times 10^{-19}$	$3.126 \times 10^{-18}$	$7.767 \times 10^{-18}$	$5.884 \times 10^{-18}$	$3.796 \times 10^{-18}$
$\bar{v}(II)/\rho$	$6.318 \times 10^{-19}$	$1.950 \times 10^{-18}$	$3.706 \times 10^{-18}$	$3.761 \times 10^{-18}$	$2.966 \times 10^{-18}$
$\bar{v}(III)/\rho$	$2.09 \times 10^{-35}$	$3.19 \times 10^{-34}$	$5.97 \times 10^{-33}$	$1.20 \times 10^{-31}$	$1.51 \times 10^{-30}$
$y$	0.603	0.574	0.548	0.576	0.214
$\frac{\bar{v}(II)(\frac{2}{3}x-1)}{\bar{v}(II)(2-y)+\bar{v}(II)y}$	0.209	0.224	0.233	0.223	0.214
$r_m/\rho$	$1.320 \times 10^{-19}$	$4.369 \times 10^{-19}$	$8.638 \times 10^{-19}$	$8.387 \times 10^{-19}$	$6.421 \times 10^{-19}$

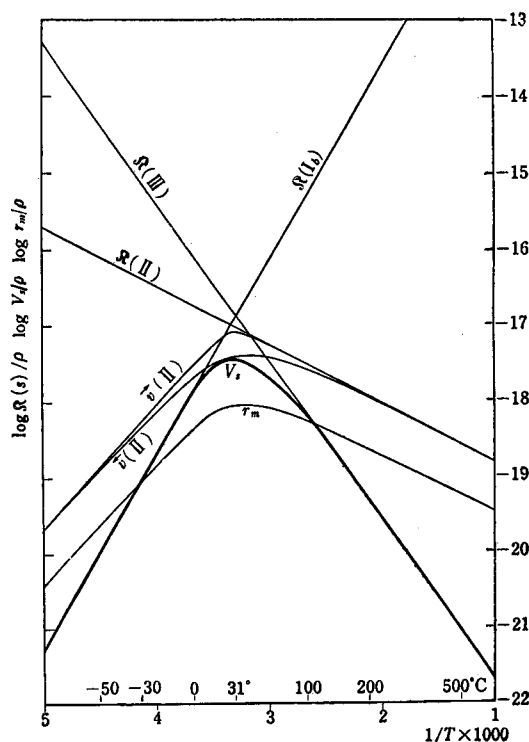


Fig. 13. Structure of hydrogenation of 1-butene.

$P_1^H = 40$  mmHg,  $P_2^H = 35$  mmHg.

below the lowest  $\mathfrak{R}(S)$  according to (12.3) and practically coincides with the latter, as the lowest  $\mathfrak{R}(S)$  grows lower than all other  $\mathfrak{R}(S)$  according to (12.4.a) and (12.1). The deviation downwards of  $V_s$  from the lowest one occurs, when more than one lowest  $\mathfrak{R}(S)$  are alike in magnitudes. Apart from  $\mathfrak{R}(I_a)$  shown to be situated high above other  $\mathfrak{R}(S)$ , the relative height of  $V_s$  is located generally as follows. If  $\mathfrak{R}(I_b)$  and  $\mathfrak{R}(III)$  are sufficiently low compared with  $\mathfrak{R}(II)$  and coincident with each other, we have  $2V_s = \mathfrak{R}(I_b) = \mathfrak{R}(III)$  from (12.6) and (11.11). The steady rate  $V_s$  deviates thus from the value of  $\mathfrak{R}(I_b) = \mathfrak{R}(III)$  by the factor 2, while it approaches the lowest value, as one of  $\mathfrak{R}(I_b)$  and  $\mathfrak{R}(III)$  increases above the other according to (12.4.a).

If  $\mathfrak{R}(I_b)$ ,  $\mathfrak{R}(II)$  and  $\mathfrak{R}(III)$  are coincident with each other, we have from (16.2)

$$(2 + r(H)) V_s = \mathfrak{R}(I_b) = \mathfrak{R}(II) = \mathfrak{R}(III).$$

This equation states that  $V_s$  deviates downwards from the common value of

$\mathfrak{R}(I_b)$ ,  $\mathfrak{R}(II)$  and  $\mathfrak{R}(III)$  by a factor  $2 + \gamma(H)$ , which lies between 2 and 3 according to (12.2). In accordance with (12.4.a), the steady rate  $V_s$  approaches the lowest  $\mathfrak{R}(S)$ , as it decreases below the other two.

Summing up,  $V_s$  is given in general by the lowest  $\mathfrak{R}(S)$  except in the case of two or three  $\mathfrak{R}(S)$  being lowest and alike in magnitudes, where  $V_s$  rounds off below the lowest  $\mathfrak{R}(S)$ -lines around their intersection as exemplified by Fig. 13.

### § 17. Rate $r_m$ of DBM Derived from the Structure

The rate  $r_m$  of DBM as well as  $y$  is calculated as shown in Table 21 from the values of  $\bar{v}(II)$  and  $\bar{v}(II)$  given in the same Table by (14.8) and (14.9), assuming that  $x$  equals the mole fraction 0.903 of 1-butene in the gas used in the present experiment.

Fig. 13 shows  $r_m$  as well as  $\bar{v}(II)$  and  $\bar{v}(II)$ . We see from the Figure that  $\bar{v}(II)$  equals  $\bar{v}(II)$  practically at sufficiently high and low temperatures, so that  $r_m = (\frac{3}{4}x - \frac{1}{2})\bar{v}(II) = 0.192\bar{v}(II)$  according to (14.16).

Fig. 13 shows, besides, that the value of  $r_m/V_s$  increases from 0 to 100°C and further from 100 to 198°C. This explains the experimental result shown in Table 14, that the composition of butenes in the product approaches to that in equilibrium with increase of the temperature. The observed intersection of the  $r_m$ - and  $r_n$ -curves shown in Fig. 9 is also reproduced by the theoretical conclusion derived from the structure in Fig. 13.

### § 18. Explanation of Experimental Results of DIBELER and TAYLOR

Fig. 14 shows the structure of hydrogenation of 1-butene constructed on the base of the value of  $\log \mathfrak{R}(S)_\infty/\rho$  calculated for the experimental condition of DIBELER and TAYLOR ( $P^H = P^B = 50$  mmHg) given in Table 22 and  $\Delta^*\epsilon(S)$  in § 15. The steady rate  $V_s$  was derived from the structure similarly as in § 16 as shown in the Figure. Fig. 14 shows that the rate-determining step switches over from  $I_b$  to III in the temperature range from 60 to 135°C of the DIBELER and TAYLOR's experiment, and accounts qualitatively for the extremely small activation energy (2.0 Kcal) observed by them as compared with that obtained by the present author (11.8 Kcal), although the activation energy is slightly negative according to the Figure at higher temperature of the range.

The order of reaction of hydrogenation is obtained by differentiating  $\ln V_s$  of (16.2) with respect to  $\ln P^H$  or  $\ln P^B$ , as

Study of the Hydrogenation and Double Bond Migration of 1-Butene on Nickel Catalyst

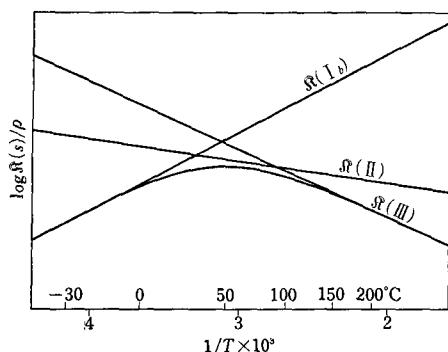


Fig. 14. Structure of hydrogenation of 1-butene.  
 $P^H = P^B = 50$  mmHg

TABLE 22.  $\log \mathfrak{K}(S)_\infty/\rho$

$P^H = P^B = 50$  mmHg

S	$\log \mathfrak{K}(S)_\infty/\rho$
I <sub>b</sub>	- 8.3251
II	- 19.3363
III	- 23.4989

$$\frac{\partial \ln V_s}{\partial \ln P^H} = - \frac{\frac{1}{\mathfrak{K}(I_b)} + \frac{\gamma(H)}{2\mathfrak{K}(II)} - \frac{\partial \gamma(H)}{\partial \ln P^H} \frac{1}{\mathfrak{K}(II)} + \frac{1}{\mathfrak{K}(III)}}{\frac{1}{V_s}} \quad (18.1.H)$$

or

$$\frac{\partial \ln V_s}{\partial \ln P^B} = \left\{ \left( \frac{\partial \gamma(H)}{\partial \ln P^B} - \gamma(H) \right) \frac{1}{\mathfrak{K}(II)} + \frac{1}{\mathfrak{K}(III)} \right\} / \frac{1}{V_s} \quad (18.1.B)$$

The differential coefficient  $\partial \gamma(H)/\partial \ln P^H$  or  $\partial \gamma(H)/\partial \ln P^B$  in the above equations is obtained by differentiating the equation

$$\frac{1}{\mathfrak{K}(I_b)(1-\gamma(H)^2)} = \frac{1}{\mathfrak{K}(I_b)} + \frac{\gamma(H)}{\mathfrak{K}(II)} + \frac{1}{\mathfrak{K}(III)}, \quad (18.2)$$

derived from (16.1) and (16.2), with respect to  $\ln P^H$  or  $\ln P^B$ , as

$$\frac{\partial \gamma(H)}{\partial \ln P^H} = \frac{\frac{1}{\mathfrak{K}(III)} - \frac{1}{\mathfrak{K}(I_b)} \frac{\gamma(H)^2}{1-\gamma(H)^2} + \frac{\gamma(H)}{2\mathfrak{K}(II)}}{\frac{1}{\mathfrak{K}(II)} - \frac{2\gamma(H)}{\mathfrak{K}(I_b)(1-\gamma(H)^2)}}, \quad (18.3.H)$$

or

$$\frac{\partial \gamma(H)}{\ln P^B} = \left( \frac{\gamma(H)}{\mathfrak{K}(II)} + \frac{1}{\mathfrak{K}(III)} \right) / \left( \frac{1}{\mathfrak{K}(II)} - \frac{2\gamma(H)}{\mathfrak{K}(I_b)(1-\gamma(H)^2)} \right) \quad (18.3.B)$$

The differential coefficient  $\partial \gamma(H)/\partial \ln P^H$  or  $\partial \gamma(H)/\partial \ln P^B$  is calculated by (18.3.H) or (18.3.B) from the values of  $\mathfrak{K}(S)$  and  $\gamma(H)$  determined similarly as in §16, hence  $\partial \ln V_s/\partial \ln P^H$  or  $\partial \ln V_s/\partial \ln P^B$  is determined by (18.1.H) or (18.1.B) as shown in Table 23 at 21 and 48°C.

TABLE 23.  $\partial \ln V_s / \partial \ln P^H$ ,  $\partial \ln V_s / \partial \ln P^B$

Temperature	$\mathfrak{R}(I_b)/\rho$	$\mathfrak{R}(II)/\rho$	$\mathfrak{R}(III)/\rho$	$r(H)$	$\partial \ln V_s / \partial \ln P^H$	$\partial \ln V_s / \partial \ln P^B$
21°C	$1.318 \times 10^{17}$	$6.026 \times 10^{16}$	$6.026 \times 10^{15}$	0.4500	0.88	0.30
48°C	$2.512 \times 10^{16}$	$1.000 \times 10^{17}$	$2.512 \times 10^{16}$	0.9062	0.66	0.89

The Table shows that both the order of reaction of hydrogenation with respect to hydrogen and butene are less than unity, which conforms qualitatively with the DIBELER and TAYLOR'S experimental results that  $V_s$  was proportional to  $(P^H)^{\frac{1}{2}}(P^B)^{\frac{1}{2}}$ .

### § 19. Explanation of Experimental Results of TWIGG

Fig. 15 illustrates the structure of hydrogenation of 1-butene appropriate to the experimental condition of TWIGG on the base of  $\log \mathfrak{R}(S)_\infty / \rho$  calculated

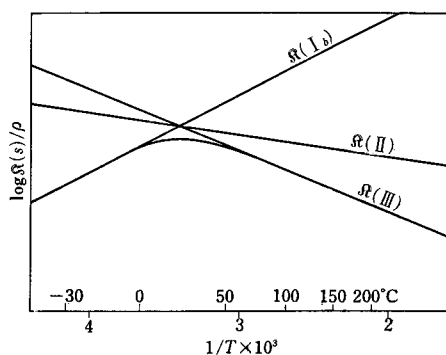


Fig. 15. Structure of hydrogenation of 1-butene.

$$P^H = P^B = 10.7 \text{ mmHg}$$

Nevertheless, the latter experimental results might be qualitatively accounted for by

TABLE 24.  $\log \mathfrak{R}(S)_\infty / \rho$   
 $P^H = P^B = 10.7 \text{ mmHg}$

$S$	$\log \mathfrak{R}(S)_\infty / \rho$
I <sub>b</sub>	- 8.9947
II	- 20.3407
III	- 24.8331

TABLE 25. Activation energy of deuteration of olefin

Olefin	Activation energy
ethene	$8.2 \pm 0.5 \text{ Kcal}$
propene	6.0
2-butenes	3.3
iso-butene	3.3

the small activation energy (2.5 Kcal) and the fractional order of reaction deduced from the structure in the neighbourhood of the optimum temperature similarly as in § 18.

TWIGG observed besides, as shown in Table 25, the activation energies of deuteration of ethene, propene and butenes on nickel catalyst between 55 and 120°C, which decreased with increase of the molecular weight. This effect may be accounted for on the basis of the structure of olefin hydrogenation as follows. The excess of the partial molal enthalpy  $\Delta^*_\varepsilon(S)$  of the critical complex over that of the appropriated set of the molecules<sup>\*)</sup> may be taken not much affected by the substituent of the hydrogen atoms of ethene, which makes the difference of olefins. The magnitudes of  $\Delta^*_\varepsilon(I_b)$ ,  $\Delta^*_\varepsilon(II)$  and  $\Delta^*_\varepsilon(III)$  determined for butene in this work approximately confirms the above expectations as compared with those for ethene<sup>8)</sup>. It is inferred on its basis that  $\mathfrak{K}(II)$  and  $\mathfrak{K}(III)$  are lowered relative to  $\mathfrak{K}(I_b)$ , without changing the relative height of  $\mathfrak{K}(II)$  and  $\mathfrak{K}(III)$ , with increase of the molecular weight of olefin, since the moment of inertia increases rapidly with increase of the molecular weight to decrease  $\mathfrak{K}(II)$  and  $\mathfrak{K}(III)$  by the same factor as seen from (15.1), (15.2) and (15.3). This factor amounts *ca.*  $2 \times 10^2$  for the transition from ethene to 1-butene as seen from Table 18. It follows as seen from Fig. 15 that the optimum temperature lowers and the inclination of  $V_s$  against  $1/T$ , *i.e.* the activation energy at a fixed temperature around the optimum decreases, in accordance with the behavior of  $V_s$  discussed in § 16, with increase of the molecular weight qualitatively in accord with the observation of TWIGG<sup>1)</sup>.

#### Acknowledgement

The author wishes to express his sincere thanks to Professor J. HORIUTI (Hokkaido University) for his kind discussion and to Professors T. SHIBA and T. KEII (Tokyo Institute of Technology) for their kind guidance.

#### [ Appendix ]

##### Order of Reaction of DBM

The order of reaction DBM has been derived in § 14 with an approximation leading to the relation that  $\bar{v}(II) = \bar{v}(II)$ . The derivation will be given below without the approximation.

The order of reaction  $\partial \ln r_m / \partial \ln P$  of DBM is developed according to (14.9) as

---

<sup>\*)</sup> Cf. § 15.

$$\frac{\partial \ln r_m}{\partial \ln P} = \frac{\partial \ln \bar{v}(\text{II})}{\partial \ln P} + \frac{\partial \ln \bar{v}(\text{II})}{\partial \ln P} - \frac{1}{\bar{v}(\text{II})(2-y) + \bar{v}(\text{II})y} \\ \times \left\{ \frac{\partial \bar{v}(\text{II})}{\partial \ln P} (2-y) + \frac{\partial \bar{v}(\text{II})}{\partial \ln P} y - \frac{\partial y}{\partial \ln P} (\bar{v}(\text{II}) - \bar{v}(\text{II})) \right\}, \quad (\text{A. 1})$$

where  $P$  is the partial pressure of reactant, *i.e.* hydrogen or 1-butene. The differential coefficients  $\partial y / \partial \ln P$ ,  $\partial \ln \bar{v}(\text{II}) / \partial \ln P$  and  $\partial \ln \bar{v}(\text{II}) / \partial \ln P$  in the above equation are expressed as follows. Differentiating (14.8) with respect to  $\ln P$ , we have

$$\frac{\partial y}{\partial \ln P} = \left\{ y(y-1) \frac{\partial \bar{v}(\text{II})}{\partial \ln P} - (2-y) \left( \frac{x}{2} - y \right) \frac{\partial \bar{v}(\text{II})}{\partial \ln P} \right\} / \\ \left\{ (2y-2-\frac{x}{2}) \bar{v}(\text{II}) - (2y-1) \bar{v}(\text{II}) \right\}. \quad (\text{A. 2})$$

Expressions of  $\bar{v}(\text{II})$  of (11.6) yield on differentiation with respect to  $\ln P$  with reference to (13.1)

$$\frac{\partial \bar{v}(\text{II})}{\partial \ln P} = \frac{\partial \mathfrak{K}(\text{II})}{\partial \ln P} \gamma(\text{H}) + \frac{\partial \gamma(\text{H})}{\partial \ln P} \mathfrak{K}(\text{II}), \quad (\text{A. 3})$$

$$\frac{\partial \bar{v}(\text{II})}{\partial \ln P} = \frac{\partial \mathfrak{K}(\text{II})}{\partial \ln P} \gamma(\text{C}_4\text{H}_9) + \frac{\partial \gamma(\text{C}_4\text{H}_9)}{\partial \ln P} \mathfrak{K}(\text{II}), \quad (\text{A. 4})$$

where  $\partial \gamma(\text{H}) / \partial \ln P$  is given by (18.3) or (18.5) for  $P \equiv P^{\text{H}}$  or  $P \equiv P^{\text{B}}$  respectively, and  $\partial \gamma(\text{C}_4\text{H}_9) / \partial \ln P$  is expressed by differentiation of the equation of the second and third member of (16.1) with respect to  $P^{\text{H}}$  or  $P^{\text{B}}$  as

$$\frac{\partial \gamma(\text{C}_4\text{H}_9)}{\partial \ln P^{\text{H}}} = \frac{\partial \gamma(\text{H})}{\partial \ln P^{\text{H}}} + \frac{1}{2} \gamma(\text{H}) - (1 - \gamma(\text{H})^2) \frac{\mathfrak{K}(\text{I}_b)}{\mathfrak{K}(\text{II})} \\ + 2\gamma(\text{H}) \frac{\mathfrak{K}(\text{I}_b)}{\mathfrak{K}(\text{II})} \frac{\partial \gamma(\text{H})}{\partial \ln P^{\text{H}}} - \frac{1}{2} \gamma(\text{C}_4\text{H}_9), \quad (\text{A. 5})$$

$$\frac{\partial \gamma(\text{C}_4\text{H}_9)}{\partial \ln P^{\text{B}}} = \frac{\partial \gamma(\text{H})}{\partial \ln P^{\text{B}}} + \gamma(\text{H}) - \gamma(\text{C}_4\text{H}_9) + 2\gamma(\text{H}) \frac{\mathfrak{K}(\text{I}_b)}{\mathfrak{K}(\text{II})} \frac{\partial \gamma(\text{H})}{\partial \ln P^{\text{B}}}. \quad (\text{A. 6})$$

The values of  $\gamma(\text{H})$  and  $\gamma(\text{C}_4\text{H}_9)$  are determined according to §16 on the one hand, and those of  $\bar{v}(\text{II})$ ,  $\bar{v}(\text{II})$  and  $y$  according to §17 on the other hand respectively for the experimental condition in question. The differential coefficient  $\partial \ln r_m / \partial \ln P^{\text{H}}$  is now evaluated for the condition by (A.5), (18.3.H), (A.3), (A.4), (A.2) and (A.1), and  $\partial \ln r_m / \partial \ln P^{\text{B}}$  by (A.6), (18.3.B), (A.3), (A.4), (A.2) and (A.1).

The order of reaction of DBM is calculated as shown in Table 26, on the base of  $x$  assumed to be the same as that in gas ( $\approx 0.903$ ), and the values

Study of the Hydrogenation and Double Bond Migration of 1-Butene on Nickel Catalyst

TABLE 26.  $\partial \ln r_m / \partial \ln P$

$P^H$ mmHg	37 (mean)	25
$P^B$ mmHg	100	58 (mean)
$\bar{n}(Ib)_{273}/\rho$	$1.254 \times 10^{-18}$	$8.471 \times 10^{-19}$
$\bar{n}(II)_{273}/\rho$	$5.023 \times 10^{-17}$	$2.395 \times 10^{-17}$
$\bar{n}(III)_{273}/\rho$	$1.888 \times 10^{-16}$	$7.402 \times 10^{-17}$
$r(H)$	0.0961	0.1275
$r(C_4H_9)$	0.0685	0.0883
$\bar{v}(II)/\rho$	$4.827 \times 10^{-18}$	$3.054 \times 10^{-18}$
$\bar{v}(II)/\rho$	$3.441 \times 10^{-18}$	$2.115 \times 10^{-18}$
$y$	0.589	0.585
$\partial \ln r_m / \partial \ln P^H$	0.44	
$\partial \ln r_m / \partial \ln P^B$		0.51

of  $P^H$  and  $P^B$  taken respectively the means in the course of experiment described in § 6.

It is shown in the Table that the calculated orders of reaction are coincident satisfactorily with observed ones, verifying that the underlying reaction scheme accounts for the experimental results.

### References

- 1) G. H. TWIGG, Trans. Faraday Soc., **35**, 934, 945 (1939).
- 2) G. H. TWIGG, Proc. Roy. Soc., **A 178**, 106 (1941).
- 3) G. H. TWIGG, Discussion of Faraday Soc., No. 8, 152 (1950).
- 4) V. H. DIBELER and T. H. TAYLOR, J. Phys. Chem., **55**, 1036 (1951).
- 5) J. HORIUTI and M. POLANYI, Trans. Faraday Soc., **30**, 663 (1934).
- 6) J. HORIUTI and M. POLANYI, Trans. Faraday Soc. **30**, 1164 (1934).
- 7) J. HORIUTI, *Shokubai (Catalysis)* **2**, 1 (1947).
- 8) J. HORIUTI, This Journal **6**, 250 (1958).
- 9) ZUR STRASSEN, Z. Physik. Chem., **A 169**, 81 (1934).
- 10) T. SHIBA, E. ECHIGOYA and T. FU, 11th Chemical Conference of the Chemical Society of Japan (1959).
- 11) J. G. ASTON and G. SZASZ, J. Chem. Phys., **14** 67 (1946).